

ERKO JAKOBSON

Spatial and temporal variability
of atmospheric column humidity

This study was carried out at the Institute of Physics, University of Tartu, Estonia.

The Dissertation was admitted on March 13, 2009, in partial fulfilment of the requirements for the degree of Doctor of Philosophy in physics (environmental physics), and allowed for defence by the Council of the Institute of Physics, University of Tartu.

Supervisor: Assoc. Prof. Hanno Ohvril, Institute of Physics, University of Tartu, Estonia

Opponents: Dr. Kalju Eerme, Tartu Observatory, Estonia
Prof. Francisco José Olmo Reyes, Granada University, Spain

Defence: 15 of May, 2009, at the University of Tartu, Estonia

ISSN 1406–0310

ISBN 978–9949–19–091–1 (trükis)

ISBN 978–9949–19–092–8 (PDF)

Autoriõigus Erko Jakobson, 2009

Tartu Ülikooli Kirjastus

www.tyk.ee

Tellimuse nr 90

CONTENTS

LIST OF APPENDED PUBLICATIONS.....	6
Author's contribution	6
OTHER PUBLICATIONS OF THE DISSERTANT.....	7
APPROBATION OF RESULTS.....	8
A LIST OF SOME OF THE ACRONYMS USED.....	10
1. INTRODUCTION.....	11
2. METHODS FOR PRECIPITABLE WATER ESTIMATION.....	13
3. ACCURACY IN RADIOSONDE MEASURED PRECIPITABLE WATER ESTIMATIONS	14
4. DATA.....	17
4.1. Radiosonde measured data	17
4.2. GPS measured data.....	17
4.3. ERA-40 reanalysis data	18
4.3.1. Moisture calculations from the ERA-40 data.....	19
4.3.2. Selection of the study period of ERA-40 data.....	20
5. SPATIAL VARIABILITY OF PRECIPITABLE WATER.....	23
5.1. Seasonal precipitable water versus latitude in the Baltic Sea region	26
5.2. Precipitable water versus surface water vapour pressure and the latitude degree in the Baltic Sea region	27
6. TEMPORAL VARIABILITY OF PRECIPITABLE WATER.....	29
6.1. Seasonal variability of precipitable water	29
6.2. Interannual variability of precipitable water.....	30
6.3. Diurnal variability of precipitable water	31
6.3.1. Regular diurnal variability	31
6.3.2. Extremal cases of the diurnal variability.....	33
7. MERIDIONAL MOISTURE FLOW.....	35
8. CONCLUSIONS.....	37
9. SUMMARIES OF APPENDED ARTICLES	40
10.SUMMARY IN ESTONIAN	43
REFERENCES.....	46
ACKNOWLEDGEMENTS	49
APPENDICES.....	51
CURRICULUM VITAE	121
CURRICULUM VITAE IN ESTONIAN	123

LIST OF APPENDED PUBLICATIONS

Journals listed in the ISI Science Citation Index are printed in **bold**.

This thesis is based on the research published in the following papers A–C and on a submitted manuscript D:

- A. Jakobson E, Ohvri H, Okulov O, Laulainen N. 2005. Variability of radiosonde-observed precipitable water in the Baltic region. ***Nordic Hydrology*** **36**: 423–433.
- B. Jakobson E, Ohvri H, Elgered G. 2009. Diurnal variability of precipitable water in the Baltic region, impact on transmittance of the direct solar radiation. ***Boreal Environmental Research*** **14**: 45–55.
- C. Vihma T, Jaagus J, Jakobson E, Palo T. 2008. Meteorological conditions in the Arctic Ocean in spring and summer 2007 as recorded on the drifting ice station Tara. ***Geophysical Research Letters*** **35**: L18706. DOI:10.1029/2008GL034681.
- D. Jakobson E, Vihma T. 2009. Atmospheric moisture budget in the Arctic based on the ERA-40 reanalysis. ***International Journal of Climatology***. Submitted.

Author's contribution

In the appended papers A, B and D, the dissertant performed most calculations, organized the preparation of the manuscript and communicated with the Editorial Boards.

In the appended paper C, the dissertant performed vertical profiles calculations and wrote the related text.

OTHER PUBLICATIONS OF THE DISSERTANT

- Rodima A, Vilbaste M, Saks O, Jakobson E, Koort E, Pihl V, Sooväli L, Jalukse L, Traks J, Virro K, Annuk H, Aruoja K, Floren A, Indermitte E, Jürgenson M, Kaleva P, Kepler K, Leito I. 2005. ISO 17025 quality system in a university environment. *Accreditation and Quality Assurance* **10**: 369–372.
- Gascard JC, Festy J, le Gogg H, Weber M, Bruemmer B, Offermann M, Doble M, Wadhams P, Forsberg R, Hanson S, Skourup H, Gerland S, Nicolaus M, Metaxin JP, Grangeon J, Haapala J, Rinne E, Haas C, Heygster G, Jakobson E, Palo T, Wilkinson J, Kaleschke L, Claffey K, Elder B, Bottenheim J. 2008. Exploring Arctic transpolar drift during dramatic sea ice retreat. *EOS, Transactions, American Geophysical Union* **89**: 21–28.
- Jaagus J, Sepp M, Jakobson E, Palo T. 2008. Atmospheric research in the Arctic realised by the Department of Geography, University of Tartu, within the DAMOCLES project. *Publicationes Instituti Geographici Universitatis Tartuensis* **107**: 88–108.
- Jakobson E, Ohvril H, Elgered G. 2007. Diurnal variability of precipitable water in the Baltic region. In: Proceedings: Fifth Study Conference on BALTEX; Kuressaare, Estonia; 4–8 June, 2007. (Eds.) Isemer, HJ. *International BALTEX Secretariat*: 119–120.
- Jakobson E, Ohvril H, Okulov O, Laulainen N. 2004. Relationships between precipitable water and geographical latitude in the Baltic region. In: Proceedings: 4th Study Conference on BALTEX; Gudhjem, Denmark; 24.–28.05.2004. (Eds.) Isemer, Hans-Jörg., 2004. *International BALTEX Secretariat*: 53–54.

APPROBATION OF RESULTS

Oral presentations

- Jakobson E, Ohvril H, Okulov O. May 2004. *Relationships between average precipitable water and geographical latitude in the Baltic region*. The Fourth Study Conference on BALTEX. Gudhjem, Bornholm, Denmark.
- Jakobson E, Ohvril H, Uustare M. March 2005. Atmosfääri veeaurusisalduse analüüs Tõraveres 2002–2004 (Analysis on atmospheric humidity content in Tõravere 2002–2004). XXXV Estonian Physics Days. Tartu, Estonia.
- Jakobson E. November 2005. Atmosfääri veeaurusisaldus, selle muutlikkus ja mõõtmise meetodid (Atmospheric humidity content variability and its measuring methods). Seminar of Meteoparameters Monitoring. Tartu, Estonia.
- Jakobson E. May 2006. Veeauru muutlikkus atmosfääris ERA-40 tagasiarvutusmudeli ning GPS-mõõtmiste põhjal (Variability in atmospheric humidity by ERA-40 reanalysis and GPS-measurements). Climate Seminar of Department of Geography. Tartu, Estonia.
- Jakobson E. November 2006. *Arktika ekspeditsioon 2006 (Arctic Expedition 2006)*. Post-graduates' Seminar of the Department of Geography. Tartu, Estonia.
- Jakobson E. December 2006. *Meteorological observations at TARA*. DAMOCLES General Assembly. Bremen, Germany.
- Jakobson E, Ohvril H, Jaagus J, Vihma T. March 2007. Atmosfääri veeaurusisalduse, meridionaalse niiskuse transpordi ja temperatuuri trendid põhjapoolkeral 1958–2001 (Trends in atmospheric humidity content, meridional moisture flow and temperature in northern hemisphere 1958–2001). XXXVII Estonian Physics Days. Tartu, Estonia.
- Jakobson E. March 2007. Meteoroloogilised mõõtmised Arktika triivjääl (Meteorological measurements in the Arctic on a pack ice). EMHI Meteorology Day Conference. Tallinn, Estonia.
- Jakobson E. May 2007. *Meteorological measurements at TARA*. DAMOCLES workgroup meeting. Copenhagen, Denmark.
- Jakobson E. May 2007. *Meteorological measurements at TARA*. Seminar of Atmospheric Physics of the Tartu Observatory. Tõravere, Estonia.
- Jakobson E. October 2007. *Tethered balloon measurements in the Arctic at drifting base TARA*. Search for DAMOCLES meeting. Paris, France.
- Jakobson E, Palo T, Jaagus J. April 2008. Meteoroloogilistest mõõtmistest Arktika triivjääl rahvusvahelisel polaaraastal (About meteorological measurements in the Arctic on pack ice during the International Polar Year). General Council of Estonian Geographical Society. Tallinn, Estonia.
- Jakobson E, Vihma T. September 2008. *On the atmospheric moisture budget in the Arctic according to ERA-40 reanalysis*. DAMOCLES workgroup meeting. Helsinki, Finland.

Poster presentations

- Jakobson E, Ohvril H, Okulov O. February 2004. Atmosfääri veesisalduse regressioonanalüüs Läänemere piirkonnas (Regression analysis on atmospheric humidity content in the Baltic Sea region). XXXIV Estonian Physics Days. Tartu, Estonia.
- Jakobson E, Ohvril H. October 2005. Atmosfääri veeaurusisaldus Tõraveres ja Tallinnas – mõõtmistulemuste võrdlus (Comparison of atmospheric humidity content measured in Tõravere and Tallinn). The Second Estonian Remote Sensing Seminar. Tõravere, Estonia.
- Jakobson E, Ohvril H. November 2005. REMO mudeli ööpäevase käigu kontroll Tõravere mõõtmistulemustega (Validation of diurnal cycle of REMO model against Tõravere measured values). Estonian Geophysics 2005. Tõravere, Estonia.
- Jakobson E, Ohvril H. April 2006. Atmosfääri veeaurusisalduse ööpäevane ja sesoonne muutlikkus Soome GPS-jaamade näitel 1998–2001 (Diurnal and seasonal variation of atmospheric humidity content based on Finnish GPS-stations, 1998–2001). XXXVI Estonian Physics Days. Tartu, Estonia.
- Jakobson E, Ohvril H, Elgered G. June 2007. *Diurnal variability of precipitable water in the Baltic region*. The Fifth Study Conference on BALTEX. Kuressaare, Estonia.
- Jakobson E, Vihma T. November 2008. *Atmospheric moisture budget over the Arctic on the basis of ERA-40 reanalysis*. DAMOCLES General Assembly. Sopot, Poland.

A LIST OF SOME OF THE ACRONYMS USED

DJF	December, January, February
GPS	Global Positioning System
IPWV, <i>W</i>	Integrated Precipitable Water Vapour, precipitable water
JJA	June, July, August
MAM	March, April, May
MMF	Meridional Moisture Flux
PtP	Peak-to-Peak
SON	September, October, November

I. INTRODUCTION

The column humidity content of the atmosphere, expressed as the integrated column of water vapour in the zenith direction, usually called integrated precipitable water vapour (IPWV), or just precipitable water (denoted W in equations and figures), is a fundamental quantity for all atmospheric sciences. The unit, mass per unit area, is in meteorological practice usually given as the thickness (height) of the layer of liquid water that would be formed if all the water vapour in the zenith direction were condensed at the surface of a unit area, hence a 1 mm layer corresponds to 1 kg/m^2 (Reitan, 1960, IPCC, 2007).

Water vapour is the most important greenhouse gas, contributing to about 60% of the natural greenhouse effect; carbon dioxide accounts for just 26%, and ozone for 8% (Maurellis and Tennyson, 2003). In contrast to other greenhouse gases, water vapour has a much higher temporal and spatial variability which is not well observed, neither is it fully understood (Jacob, 2001, Wagner *et al.*, 2006).

Water vapour strongly modulates the propagation of solar and terrestrial radiation and plays a crucial role in the Earth's radiation budget. Besides this, water vapour also has a significant influence on the accuracy of satellite monitoring information regarding surface properties (satellite images), GPS applications, describing hydrological cycle, analysis of transmittance of the direct solar radiation, etc.

Changes in the atmospheric moisture budget as well as cloud coverage and properties belong to key factors controlling the strength of future Arctic climate change (Sorteberg *et al.*, 2007). Accurate information on the air moisture is also essential for monitoring the Arctic climate: uncertainties in the water vapour content cause errors in satellite-based observations on the surface temperature, albedo (Aoki *et al.*, 1999) and sea ice concentration (Kaleschke *et al.*, 2001).

During recent decades, a strong improvement has been witnessed in the accuracy of atmospheric model analyses, re-analyses, and forecasts (Simmons and Hollingsworth, 2002, Uppala *et al.*, 2005). Due to changes in models and data assimilation systems, operational analyses do not provide a consistent long-term data set on the atmospheric moisture budget. Reanalyses, however, based on the utilization of the same model and data assimilation procedure, are better in this respect. The potential of reanalyses in investigations of the Arctic moisture budget was realized by Walsh *et al.* (1994) already before the first reanalyses became available. Several reanalyses are presently available. Motivation for selecting ERA-40 reanalysis for the present study is given in Section 2.1 of the appended publication D.

The objective of this thesis is to present:

- accuracy estimation for radiosonde measured precipitable water;
- comprehensive picture of spatial and temporal variability of precipitable water in the Baltic Sea region and, more generally, the region northward 55°N ;

- overview of humidity transport in the region northward 55°N;
- regional trends in IPWV in the region northward 55°N;
- trends for IPWV averages and related parameters of the region northward 70°N.

This thesis is organized as follows. Chapter 2 gives a short overview of available methods for precipitable water estimation. In Chapter 3, accuracy estimation for radiosonde measured precipitable water is given. In Chapter 4, an overview of used databases and calculation equations are given. Chapter 5 discusses the spatial variability of precipitable water, both for the Baltic Sea region and for the region north of 55°N. A parameterization equation for the Baltic Sea region using surface water vapour pressure is given. Interannual and diurnal variability of precipitable water is discussed in Chapter 6. Chapter 7 comprises the moisture meridional flow, Chapter 8 contains conclusions, Chapter 9 summarizes the appended publications and Chapter 10 contains summary in Estonian.

2. METHODS FOR PRECIPITABLE WATER ESTIMATION

The oldest and most fundamental method for the IPWV measurements is integration of radiosonde vertical humidity profiles. Radiosondes have been used for a long period and in principle, a long continuous data set is available. However, it should be noted that the changes in the radiosondes humidity sensors diminish the continuity of the IPWV time series from about 1980 backwards. In reanalyse models, timeseries of older types of humidity sensors are adjusted.

The number of measurement techniques for observations of IPWV increased considerably in the 1990s and now includes ground-based and space-borne optical soundings and microwave radiometry, as well as propagation delay estimation using ground-based GPS data. The modern techniques enable a high temporal resolution (from seconds to minutes). It has been shown that GPS, radiosonde and microwave radiometer measurements of IPWV are in reasonable agreement with each other (Bouma and Stoew, 2001, Gldner, 2001, Dai *et al.*, 2002).

The amount of precipitable water has significant correlation with several meteorological parameters measured near the underlying surface: partial pressure of water vapour, dew-point temperature, air temperature, relative humidity, etc. Simple linear regression with partial pressure of water vapour gives the best approximation for the IPWV in Estonia, Tallinn (Okulov *et al.*, 2002).

3. ACCURACY IN RADIOSONDE MEASURED PRECIPITABLE WATER ESTIMATIONS

In this chapter, the uncertainty of the IPWV is estimated, measured by the modern Vaisala RS 90 sensor. Uncertainty estimation is made according to the ISO Guide to the Expression of Uncertainty in Measurement (abbreviated GUM) (Kirkup and Frenkel, 2006).

Precipitable water W is defined as:

$$W = \int_{z_0}^{z_1} a(z) \cdot \delta z \approx \sum_i a(z_i) \cdot \Delta z_i, \quad (3.1)$$

where $a(z)$ is absolute humidity at an altitude z . This equation is equal with equation

$$W = \frac{1}{g} \int_{p_0}^{p_1} q(p) \cdot \delta p \approx \frac{1}{g} \sum_i q(p_i) \cdot \Delta p_i, \quad (3.2)$$

where g is acceleration due to the gravity and $q(p)$ is specific humidity at a pressure level p . The W content in a vertical interval Δp_i is:

$$\Delta W_i = \frac{1}{g} q(p_i) \cdot \Delta p_i. \quad (3.3)$$

Standard uncertainty $u(\Delta W_i)$ of the humidity content ΔW_i in the interval Δp_i is:

$$u(\Delta W_i) = \Delta W_i \sqrt{\left(\frac{u(q(p_i))}{q(p_i)} \right)^2 + \left(\frac{u(\Delta p_i)}{\Delta p_i} \right)^2}. \quad (3.4)$$

Next an assumption is made that difference in the specific humidity is negligible between pressure levels p_i and $p_i + u(p_i)$. Consequently, summation over the whole vertical profile does not depend on the actual vertical location of levels, so it can be stated that

$$u(\Delta p_i) = 0, \quad (3.5)$$

and equation (2.4) reduces to a simple form:

$$\frac{u(\Delta W_i)}{\Delta W_i} = \frac{u(q(p_i))}{q(p_i)}. \quad (3.6)$$

Next an assumption is made that the relative uncertainty in specific humidity is constant in the whole profile. Thus the relative uncertainty in the precipitable water is equal to the relative uncertainty in the specific humidity:

$$\frac{u(W)}{W} = \frac{\sum_i u(\Delta W_i)}{\sum_i \Delta W_i} = \frac{\sum_i \Delta W_i \cdot \frac{u(q(p_i))}{q(p_i)}}{\sum_i \Delta W_i} \approx \frac{u(q(p_i))}{q(p_i)}. \quad (3.7)$$

Specific humidity q (kg/kg) is given as:

$$q(e, p) = \frac{0.622 \cdot e}{p - 0.378 \cdot e}, \quad (3.8)$$

where the water vapour pressure e and barometric pressure p are in hPa. Standard uncertainty of specific humidity $u(q)$ is:

$$u(q) = \sqrt{\left(u(e) \cdot \frac{\partial}{\partial e} q(e, p)\right)^2 + \left(u(p) \cdot \frac{\partial}{\partial p} q(e, p)\right)^2}. \quad (3.9)$$

Saturated water vapour pressure depends on whether it is calculated with respect to water or with respect to ice. According to the World Meteorological Organization (WMO) suggestion (WMO, 1988), the saturated water vapour pressure is calculated at all temperatures with respect to water. For water vapour pressure e (hPa) calculation the Magnus type equation (Aruksaar *et al.*, 1964) of temperature T (K) and relative humidity RH is used:

$$e(T, \text{RH}) = 6.1078 \cdot 10^{\frac{7.567 \cdot T - 2066.92805}{T - 33.45}} \cdot \text{RH}. \quad (3.10)$$

Standard uncertainty $u(e)$ of water vapour pressure is:

$$u(e) = \sqrt{\left(u(T) \cdot \frac{\partial}{\partial T} e(T, \text{RH})\right)^2 + \left(u(\text{RH}) \cdot \frac{\partial}{\partial \text{RH}} e(T, \text{RH})\right)^2}. \quad (3.11)$$

The manufacturer of the Vaisala RS 90 sensors has estimated the standard uncertainties in atmospheric pressure p , temperature T and relative humidity RH as follows (Antikainen *et al.*, 2002):

$$u(p) = 0.75 \text{ hPa}, \quad u(T) = 0.25 \text{ K}, \quad u(\text{RH}) = 2.5\%. \quad (3.12)$$

For example, assuming fixed conditions

$$p = 1000 \text{ hPa}, \quad T = 10^\circ \text{C}, \quad \text{RH} = 70\%, \quad (3.13)$$

water vapour pressure $e = 8.59$ hPa and its standard uncertainty $u(e) = 0.34$ hPa; specific humidity $q = 5.36$ g/kg and its standard uncertainty $u(q) = 0.21$ g/kg. According to Equation 3.7, relative standard uncertainty in the precipitable water is $u(W)/W = 0.04$ and the relative expanded uncertainty in the precipitable water at 95% confidence level is 8% (2 mm for average value IPWV = 25 mm).

The uncertainty depends on relative humidity rather than on temperature. For relative humidity $RH = 90\%$, the relative expanded uncertainty in IPWV is 7%, but for $RH = 30\%$, the relative expanded uncertainty in IPWV is 17%. in comparison, GPS measured IPWV expanded uncertainty at 95% confidence level is also estimated to be 2 mm (Emardson *et al.*, 1998, Tregoning *et al.*, 1998).

4. DATA

This thesis is based on the three IPWV databases:

- radiosonde measured data,
- GPS measured data,
- ERA-40 reanalysis data.

4.1. Radiosonde measured data

Night-time radiosonde reports at 00 UTC from 17 aerologic stations from 1989 to 2002 in the Baltic Sea region were used to obtain values of IPWV. The northernmost site, the Finnish station at Sodankylä (67.37°N), is located just beyond the polar circle (66.6°N), while the southernmost location, the Polish station at Wroclaw (51.79°N), is situated 15.58° (1730 km) southward. Actually, there are more stations in this region (e.g. Pskov), but they were excluded because their time series are too inhomogeneous or short, or they do not have observations at 00 UTC. Radiosondes are usually launched twice daily, at 00 UTC and 12 UTC. We omitted the 12 UTC because the set of 12 UTC soundings is less complete and the diurnal cycle of IPWV is usually weak compared to the overall value of IPWV (Güldner and Spänkuch, 1999). The practice to confine the analysis to 00 UTC observations has also been applied by Ross *et al.* (2002), who examined radiosonde data for 150 stations in the USA and Canada.

In this work, sounding profiles in the low vertical resolution WMO TEMP format were used, accessible for public use at the website of the University of Wyoming (<http://www.uwyo.edu>). Soundings with at least 14 levels were considered; usually 15–30 levels were represented. For each sounding, precipitable water is already calculated and presented on the website. The author of the present thesis found that the relative difference due to the use of low vertical resolution data instead of high vertical resolution data (100–500 observational levels) in numerical vertical integration is usually less than 2%, thus less than the error of the device.

4.2. GPS measured data

GPS measured data used in this paper was gathered from 21 Swedish stations (SWEPOS) from 1996 to 2005, 10 Finnish stations (FINNREF) from 1997 to 2005 and 1 Latvian station (Riga) from 1998 to 2005. This dataset was produced by Lidberg *et al.* (2007) with temporal resolution of 2 hours. For case studies of fast IPWV variations at Onsala (Sweden), a dataset produced by Johansson *et al.* (2002) with temporal resolution of 5 minutes was used.

The part of the zenith total delay (ZTD) caused by water vapour, the zenith wet delay (ZWD), was derived by subtracting the so-called zenith hydrostatic delay (ZHD) using values of the ground pressure interpolated from a numerical weather analysis as described by Gradinarsky *et al.* (2002). The conversion from ZWD to the IPWV used the model presented by Emardson and Derks (2000) which is based on the season (day of year) and the latitude of the site. The uncertainties in the GPS-measured IPWV values have many origins and span from white noise in fundamental carrier-phase observations to long term bias effects due to uncertainties in physical constants used in the conversions described above. A total root-sum-square error of GPS measured IPWV has been shown to be slightly above the 1-mm (Emardson *et al.*, 1998, Tregoning *et al.*, 1998).

4.3. ERA-40 reanalysis data

During recent decades, a strong improvement in the accuracy of atmospheric model analyses, re-analyses, and forecasts has been witnessed (Simmons and Hollingsworth, 2002, Uppala *et al.*, 2005). Due to changes in models and data assimilation systems, operational analyses do not provide a consistent long-term data set on the atmospheric moisture budget. Reanalyses, however, based on the utilization of the same model and data assimilation procedure, are better in this respect.

ERA-40 reanalysis data is produced by European Centre for Medium-Range Weather Forecasts (ECMWF). The ERA-40 reanalysis covers 44 full years from 1958 to 2001, and is based on a forecast model at a T159 resolution (approximately 125 km in the horizontal). The temporal resolution is 6 h and the vertical resolution is 60 levels, more than half of which are in the troposphere. In this study, data from the lowest 27 levels of ERA-40 was applied (even after reducing, the raw data amount is more than 100 GB). The uppermost one is approximately at 300 hPa pressure level (about 9 km). The author of this thesis learned that the error caused by the reduced number of levels is about 1% for the vertically integrated water vapour.

Specific humidity and northward wind for 27 lower levels and surface pressure were collected directly from the ECMWF data archive in a 1° by 1° grid covering the region 55–90°N. Air pressure at higher levels was calculated by ERA-40 model algorithm from surface pressure. IPWV and Meridional Moisture Flux (MMF) seasonal averages were calculated for each grid point for each level to fasten the following calculations. The area averages were calculated separately for the polar cap, 70–90°N, which allowed the author to compare the results directly with many previous studies.

The water vapour data assimilated into ERA-40 are humidity profiles from radiosondes and, since 1979, raw radiances from a number of satellite instruments, e.g., the Vertical Temperature Profile Radiometer (VTPR) and

Special Sensor Microwave Imager (SSM/I) on board NOAA satellites and the High Resolution Infrared Radiation Sounder (HIRS/2 and HIRS/3) from both the TIROS Operational Vertical Sounder (TOVS) and Advanced TOVS (ATOVS). Bromwich *et al.* (2002, 2007) reported a systematic cold bias in ERA-40 over the Arctic during 1979–1996 due to assimilation of the High Resolution Infrared Radiometer (HIRS) data. The largest bias coincides with locations of sea ice. The bias was more pronounced in summer, and may have contributed to the anomalously high summer precipitation in the central Arctic (Serreze and Etringer, 2001).

This study concentrates on water vapour; cloud liquid water and ice are not included. In polar regions, as an annual average, water vapour represents approximately 99% of the total water content (vapour, liquid, and ice) in the atmosphere (Tietäväinen and Vihma, 2008).

Over snow- and ice-covered regions, remote sensing data on air humidity were, however, not assimilated to ERA-40. This is due to the difficulties in distinguishing between the signals originating from the surface and the atmosphere. In the model, a fractional sea ice cover is allowed for each grid cell; the sea ice concentration is based on satellite measurements from the Special Sensor Microwave Imager (SSM/I) using two-dimensional variational data assimilation (Fiorino, 2004). The ice thickness is prescribed as 1.5 m, but there is no snow on top of the ice. The surface albedo is, however, prescribed to have a seasonal cycle typical of the snow albedo. Over the Arctic, the effects of data assimilation on the ERA-40 wind field arise from the surface pressure observations from drifting buoys and terrestrial stations, as well as from the satellite-based temperature profile data. With many new measurement campaigns in the Arctic during the International Polar Year from March 2007 to March 2009, there is big hope to improve models. For example, within DAMOCLES (Developing Arctic Modelling and Observing Capabilities for Long-term Environmental Studies), the atmospheric boundary layer vertical profiling with tethered sonde is a unique material for model validations (Gascard *et al.*, 2008, Vihma *et al.*, 2008).

4.3.1. Moisture calculations from the ERA-40 data

To calculate the total water vapour content, IPWV, numerical integrations of specific humidity, q (kg/kg) through an atmospheric column were made from surface pressure, p_1 , to the 27th level pressure, p_{27} :

$$W = -\frac{1}{g} \sum_{i=p_1}^{p_{27}} q_i \, dp_i , \quad (4.1)$$

where g is the acceleration due to gravity.

For the vertically numerically integrated meridional moisture flux MMF ($\text{kg m}^{-1} \text{s}^{-1}$):

$$\text{MMF} = -\frac{1}{g} \sum_{i=p_1}^{p_{27}} q_i \cdot v_i dp_i, \quad (4.2)$$

where v is the northward wind speed component.

4.3.2. Selection of the study period of ERA-40 data

The time series of the annual averages over the polar cap (70–90°N) of IPWV and four closely related atmospheric parameters (2 m air temperature t , precipitation P , evaporation E , and net precipitation $P-E$) are presented in Figure 1. The time series were divided in two periods: before the era of satellite data assimilation (1958–1978) and during the satellite era (1979–2001), and used the F-test to study the statistical significance of the linear trends. Coefficients of determination (R^2) between the year and the variables (annual averages over the polar cap) are presented in Figure 1, and trends of the time-series are presented in Table 1.

For the whole period (1958–2001), the trends of all variables, except IPWV, are statistically significantly (95%) positive (Table 1). Before the satellite era, the trends in the IPWV, precipitation and net precipitation are statistically significantly positive, while there is no significant trend in air temperature and evaporation. During the satellite era, the only significant trend is found in the 2 m air temperature. Previous studies based on ERA-40 for partly different regions have indicated that there is no significant trend in IPWV for 1958–2001 at 60–90°N (Rinke *et al.*, 2008), and no significant trend in the net precipitation over the Arctic Ocean in 1979–2001 (Serreze *et al.*, 2006). The change in the trends is supposedly caused by the change in the data assimilated to the model, as before 1979 there were no satellite data.

Trend assessments from reanalysis are fraught with uncertainty (Trenberth *et al.*, 2005, Trenberth and Smith, 2006, Serreze *et al.*, 2007), and instead of quantifying trends, our purpose is to eliminate periods for which ERA-40 is not reliable enough. Trends in the study quantities show remarkable changes around 1979, simultaneously with the beginning of assimilation of satellite data. The author cannot be sure how large a portion of these changes can be explained by the assimilation of satellite data and by decadal changes in the large-scale atmospheric circulation, and therefore adopted a careful approach and included in the analyses data from 1979 to 2001 only.

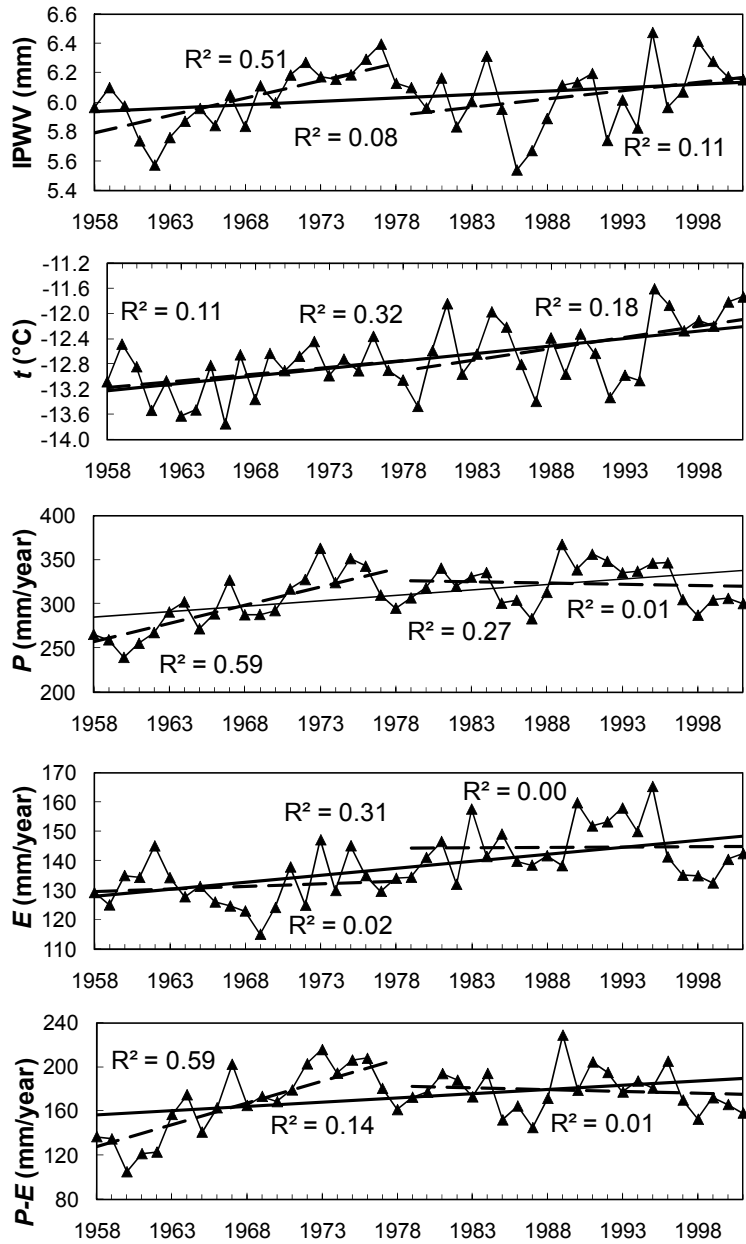


Figure 1. Time series of the annual averages of the IPWV (mm), 2 m air temperature t (°C), precipitation P (mm/year), evaporation E (mm/year), and net precipitation $P-E$ (mm/year) for polar cap (70–90°N). The coefficient of determination (R^2) is marked for periods 1958–1978, 1958–2001, and 1979–2001.

Table 1. Trends of time series of annual average IPWV, 2 m air temperature, precipitation, evaporation and net precipitation over polar cap (70–90°N). Statistically significant (95% confidence level) trends are marked in bold

Variable	Unit	1958–1978	1979–2001	1958–2001
IPWV	mm	0.024	0.011	0.005
Temperature	°C	0.021	0.035	0.024
Precipitation	mm/year	4.090	–0.311	1.238
Evaporation	mm/year	0.175	0.035	0.476
Net precipitation	mm/year	3.915	–0.346	0.761

5. SPATIAL VARIABILITY OF PRECIPITABLE WATER

The average planetary mass of atmospheric water vapour is estimated to be $13.1 \cdot 10^{15}$ kg (Peixoto, 1992). Dividing it by the Earth surface area, the planetary average value of precipitable water is $IPWV = 25$ mm. In Estonia the $IPWV$ values range from about 1 mm (cold dry winter weather) to about 40 mm (warm damp weather). For comparison, in Calcutta (South India, $22.66^{\circ}N$, $88.46^{\circ}E$), the maximal value of $IPWV = 94.9$ mm was observed on 16 July 2003.

Spatial variability in the precipitable water generally depends on the latitude. This is due to the northward decrease in air temperature, which controls the atmospheric capacity to contain water vapour. In addition, spatial variability depends on orography, continentality, underlying surface type (land, water or ice), atmospheric circulation, the properties of the underlying surface, etc.

Intergovernmental Panel on Climate Change (IPCC, 2007) states that water vapour concentration in the atmosphere mainly depends on air temperature. The authors of this thesis calculated seasonal correlations between surface temperature and $IPWV$ and found that from ERA-40 data the relation does not apply to all seasons and all regions. In autumn and winter, the correlations were quite high, with average correlation $R = 0.8$ and minimal correlations still $R = 0.5$. In spring and summer, the correlations were smaller, with average correlation in spring $R = 0.7$ and in summer $R = 0.6$. Minimal correlations were in summer even slightly negative, for example in Labrador Sea. Still, further conclusions on this topic cannot be made, as there is cold bias in ERA-40 over the Arctic from 1979 to 1996 (Bromwich *et al.*, 2002, Bromwich *et al.*, 2007). For analyzing connection between $IPWV$ and temperature, better databases are needed.

Summer $IPWV$ distributions in the Baltic Sea region from both radiosonde and GPS measurements are presented in Figure 2. Radiosonde measurements were taken from 1989 to 2002 from 17 stations, and GPS measurements from 1996 to 2005 from 32 stations. The distribution of radiosonde stations is very sparse and most of the stations are close to the sea, so the corresponding isolines do not describe well the differences between inland areas and shore areas. The distribution of GPS stations in Sweden and Finland is reasonably dense. In Figure 3 $IPWV$ seasonal distribution is presented in the region $55\text{--}70^{\circ}N$ and $3\text{--}33^{\circ}E$ from ERA-40 reanalysis taken from 1979 to 2001. Summer isolines, calculated by all three methods (radiosonde, GPS, ERA-40), are in reasonably good agreement with each other; major discrepancies occur with radiosonde data, supposedly due to the sparse distribution near the Gulf of Bothnia. The agreement between reanalysis data and measured data gives proof to the correctness of ERA-40 reanalysis $IPWV$ in the Baltic Sea region and enables to analyze $IPWV$ spatial variability on the basis of ERA-40 data only.

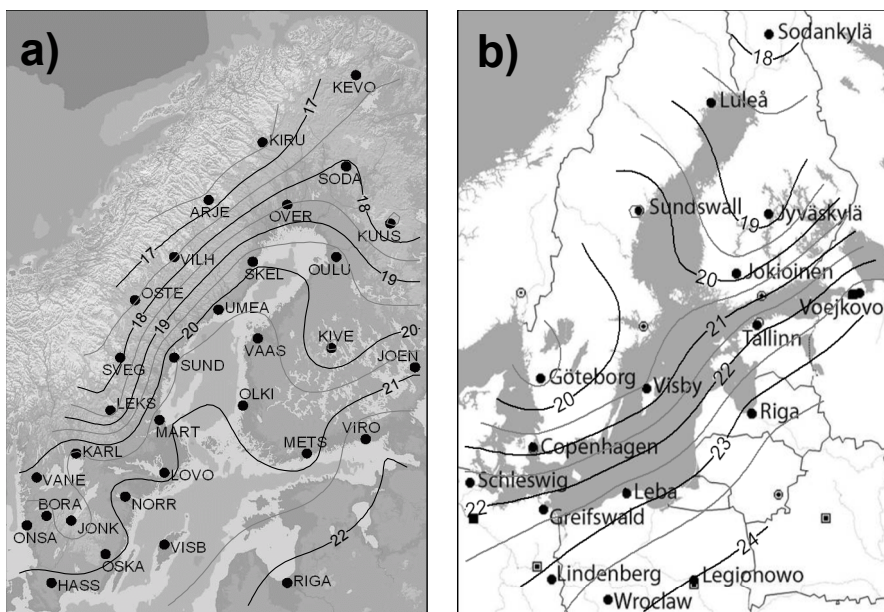


Figure 2. The summer (JJA) IPWV (mm) isolines for the Baltic Sea region from (a) radiosonde measurements and (b) GPS measurements.

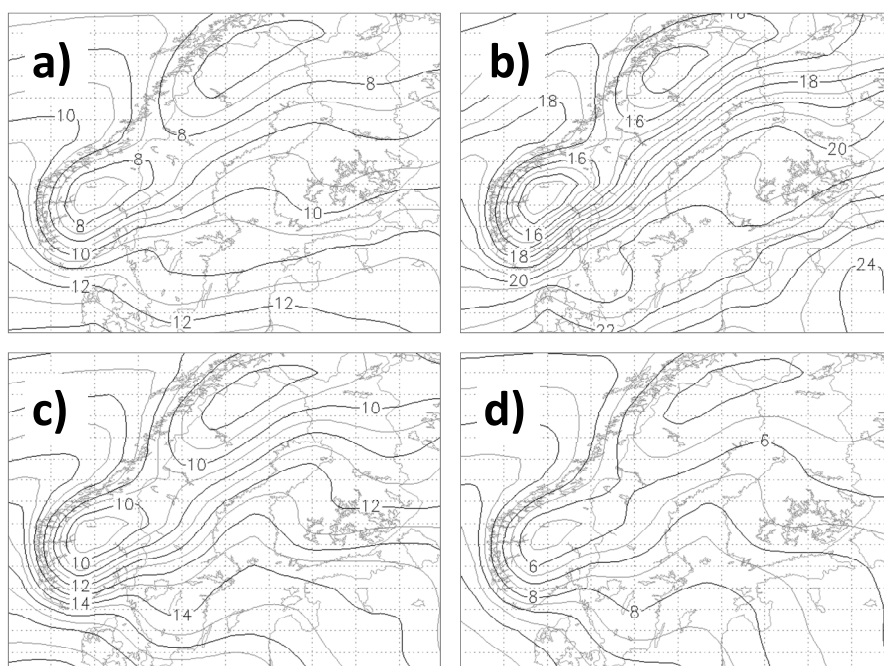


Figure 3. Seasonal IPWV (mm) isolines for the Baltic Sea region from the ERA-40 reanalysis for (a) MAM, (b) JJA, (c) SON and (d) DJF.

The minimal IPWV values occur in the highest areas of the Scandinavian Mountains (up to 2469 m) with IPWV summer average values less than 14.5 mm and winter average values less than 5 mm. In summer, the maximal average IPWV exceeds 24 mm in the more continental south-eastern part of the region. In winter and autumn, the maximal average IPWV values exceed 10.5 and 17 mm respectively in the more maritime south-western part of the region. In the radiosonde measurements area, the isolines are quite zonal and uniformly distributed, which enables the calculation of the seasonal averages in the region only from latitude (analyzed in section 5.1).

In all seasons, the IPWV isolines in the Scandinavian Mountains comply with orography well, with lower values at higher altitudes. In lower regions (above water, the Baltic states, Finland, southern Sweden), the isolines' shape is controlled by latitude and also by the continentality of the area and the type of underlying surface. The IPWV in the Atlantic sector increases due to the heating effect of the North Atlantic Current in colder seasons. The difference in the location of the maximum IPWV seasonal average can be explained with the difference in the continentality. In the Atlantic sector, the annual temperature range is fairly small (Serreze and Barry, 2005). Accordingly, IPWV range there is also small. For that reason, summer values in IPWV are smaller than in more continental areas at the same latitude, while winter values are higher than in more continental areas.

Seasonal distribution of IPWV for the region of 55–90°N from 1979 to 2001 is presented in Figure 4. Naturally, IPWV values decrease towards Pole. The isolines of IPWV are prolonged in the Canada-Siberia axis during all seasons, with the maximum asymmetry in winter, while the heat and moisture sources in the Atlantic and Pacific Oceans ensure the high level of IPWV. In summer, the asymmetry decreases due to enhanced evaporation over warm land surfaces (Walsh *et al.*, 1994). Higher values are in the Atlantic sector; only in summer, the highest values along a latitudinal belt occur in continental Europe and western Asia. The smallest values are in Greenland, where the average value of IPWV is below 4 mm even in summer. This is due to the high altitude with low temperatures.

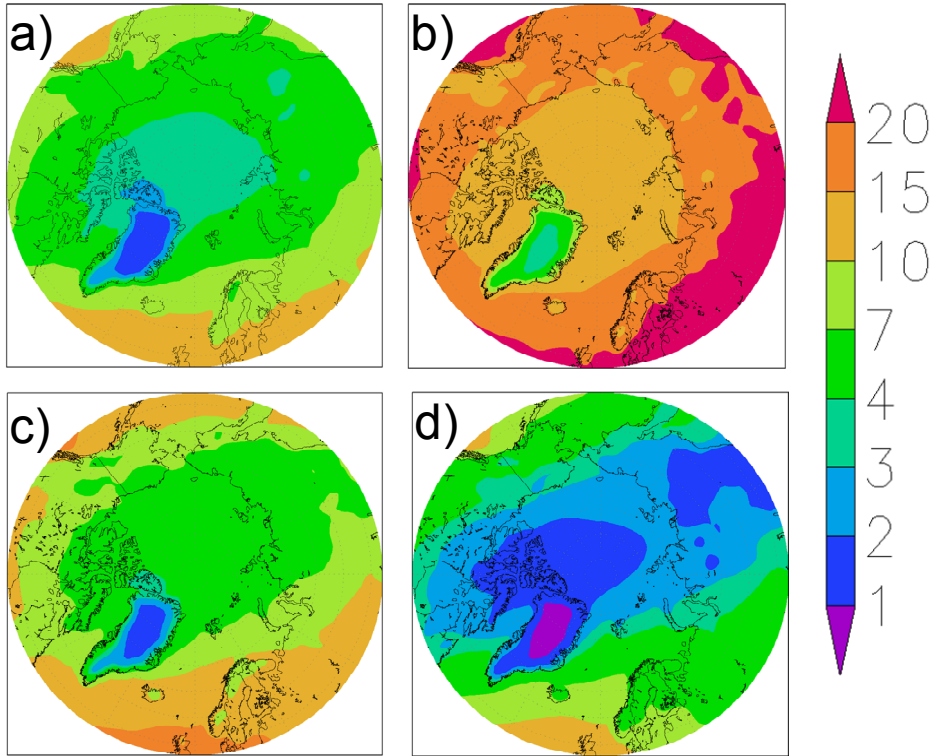


Figure 4. Seasonal averages of IPWV (mm) from ERA-40 reanalysis for 1979–2001 for (a) MAM, (b) JJA, (c) SON and (d) DJF.

5.1. Seasonal precipitable water versus latitude in the Baltic Sea region

In order to study the southward increase of precipitable water, radiosonde measured IPWV values were averaged over the four seasons: spring (MAM), summer (JJA), autumn (SON) and winter (DJF). Apparently, due to the relatively small north–south extent of the Baltic Sea region, a simple linear fit was found to express the dependence of seasonal averages of IPWV on the latitude degree φ . A linear expression for each season is given in Figure 5. Scatter of seasonal averages from the linear fit is greatest in summer and winter (coefficient of determination $R^2 = 0.67$ and 0.86 respectively). During these seasons, the proximity of two different environments – oceanic and continental – especially affects the properties of air, resulting in deviation from the average latitudinal trend. Another factor affecting humidity is the extent of the Baltic Sea in the meridional and zonal directions, which precludes uniform spatial variations of air temperature and humidity in the region (Mietus, 1998). In

February the intensity of average air flow over the Baltic Sea region starts to decrease. In April and May, due to the weakened Icelandic Low, the Atlantic air flow is very weak, the pressure pattern above the area becomes irregular and air moves even from east to west (Mietus, 1998). The atmosphere over the region is well mixed and the latitudinal trend describes meridional changes of IPWV with high rate of determination ($R^2 = 0.93$). Autumn (SON) in the Baltic Sea region is characterised by strong winds (Mietus, 1998). The atmosphere over the region is again well mixed and a linear trend describes meridional changes of IPWV with high rate of determination ($R^2 = 0.94$).

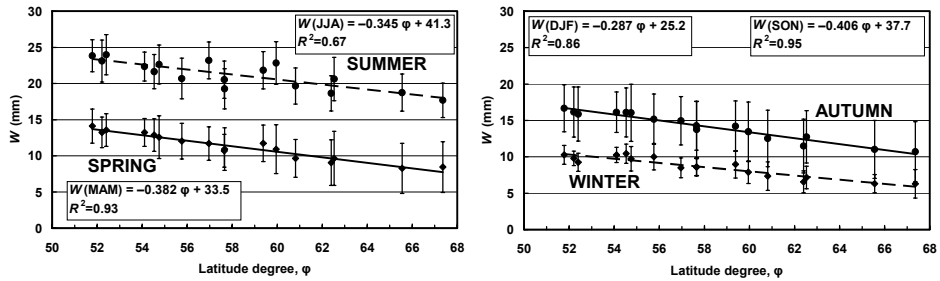


Figure 5. Average seasonal precipitable water as a function of geographical latitude ϕ , 1989–2002. Error bar is standard deviation between single monthly averages and average seasonal value. The linear equations between latitude ϕ and seasonal average precipitable water are given. Coefficient of determination R^2 evaluates applicability of the linear formula.

5.2. Precipitable water versus surface water vapour pressure and the latitude degree in the Baltic Sea region

According to an analysis performed by Okulov *et al.* (2002), a linear expression between IPWV and midday (12 UTC) surface water vapour pressure e_0 ,

$$\text{IPWV} = a e_0 + b, \quad (5.1)$$

appeared to be the best fit between precipitable water and surface humidity parameters in Tallinn. The author generalised this result for the Baltic Sea region considering coefficients a and b as linear functions of latitude ϕ . The coefficients were found by applying the least square method to more than 60 000 soundings from 17 stations during 1989–2002:

$$a = -0.0089\phi + 2.16, \quad (5.2)$$

$$b = 0.132\phi - 7.4, \quad (5.3)$$

which leads to a two-parameter all-seasons formula for the approximate calculation of single values of the IPWV:

$$\text{IPWV} = 2.16e_0 - 0.0089 e_0\varphi + 0.132 \varphi - 7.4, \quad (5.4)$$

where the IPWV is in mm, e_0 is the midnight (00 UTC) surface water vapour pressure in hPa and φ is latitude in degrees. Using this formula, standard deviations in IPWV are only 3.3–4.6 mm (18–22%) in summer, 2.6–4.0 mm (23–25%) in autumn, 2.4–3.4 mm (21–28%) in spring and 2.0–3.4 mm (31–34%) in winter.

6. TEMPORAL VARIABILITY OF PRECIPITABLE WATER

6.1. Seasonal variability of precipitable water

Average values of IPWV from ERA-40 data for polar cap (70–90°N) are 4.0 mm in spring, 12.3 mm in summer, 5.5 mm in autumn and 2.4 mm in winter, so there is more than 5 times difference in summer and winter average values.

Seasonal variability in IPWV strongly depends on the location (Figure 6a). Higher variability (summer average more than 5 times the winter average) takes place in a region covering Canada except the Rocky Mountains, the Arctic Ocean and Siberia. The variability is highest – more than 11 times – in the region south of Yakutsk, where in summer the average value exceeds 20 mm, while in winter the average value is 1–2 mm. Smaller (less than 5 times) variability occurs over the Atlantic Ocean, Europe, southern Greenland, the Bering Sea, Alaska, and the Rocky Mountains in Canada. The variability is smallest – less than 2 times – in the Scottish region, where all seasonal averages are in the range of 10–20 mm. The IPWV mean values are fairly similar in the transition seasons: in the whole study area, the autumn values are 1.3 ± 0.2 times higher than the spring ones (Figure 6b). This shows that local factors, such as latitude, altitude, and surface type do not play a significant role for the autumn and spring ratio in IPWV (in contrast to the summer and winter ratio).

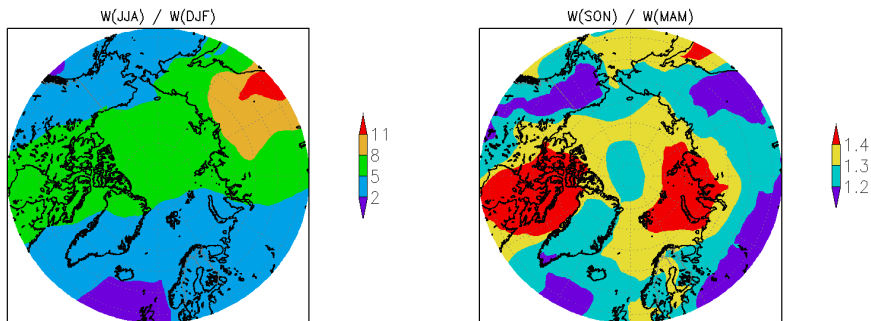


Figure 6. (a) Summer precipitable water $W(JJA)$ divided by winter $W(DJF)$ and (b) autumn precipitable water $W(SON)$ divided by spring $W(MAM)$. Note the differences in the scales.

6.2. Interannual variability of precipitable water

Interannual standard deviations in IPWV from ERA-40 data are presented in row 2, Figure 7 and are quite similar to the IPWV seasonal average maps (row 1, Figure 7). In most regions, coefficients of variations of IPWV (row 3, Figure 7) range from 5% to 10% in summer and from 10% to 20% in winter.

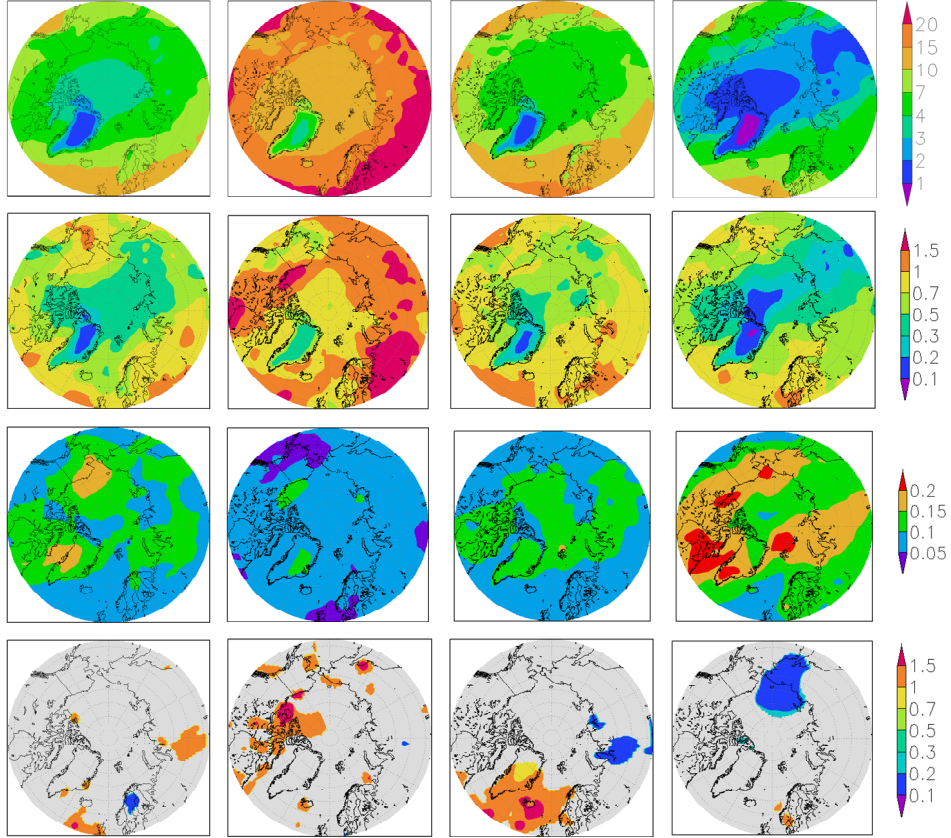


Figure 7. Seasonal values of (row 1) precipitable water IPWV (mm), (row 2) interannual seasonal standard deviation of IPWV (mm), (row 3) coefficient of variation of IPWV and (row 4) statistically significant trend in IPWV. Columns correspond to seasons (MAM, JJA, SON and DJF). All calculations apply to the period of 1979–2001.

There is no significant trend (at the confidence level 95%) in the time series of the annual averages of IPWV over the polar cap (70–90°N) (Figure 1). However, there are regions with significant trends. Statistically significant seasonal trends in IPWV at the confidence level 95% are presented in row 4, Figure 7. Areas without significant trend are given in grey; significantly

positive trends are given in red colours and significantly negative areas in blue colours. Most of the areas with significant trends are small and it is not certain whether these trends reflect real processes or are artificially produced by reanalysis process. Larger areas with significantly positive trend are in summer in the Queen Elizabeth Islands and in autumn in the North Atlantic Ocean and Southern Greenland. Larger significantly negative trend area is in Chukotka and the Chukchi Sea. Both positive and negative trends are mostly in range of 0.02 to 0.1 mm per year. The positive trends are quite small compared to the average values in these regions. Winter negative trend is, however, relatively very big, as change during the analyzed 23 years is in range of 0.5 to 2.3 mm, that is in the same order with the region winter average – in range 2 to 4 mm. For further conclusions, this result should be validated against measured values or some other reanalysis data.

6.3. Diurnal variability of precipitable water

Factors influencing the diurnal changes of IPWV are divided into two groups. The fast and extensive but irregular IPWV variations are due to changes in synoptic situation and the substitution of air masses above the GPS site leading to rapid and large (more than 10 mm) variations in the vertical profiles of water vapour. However, these kind of abrupt changes are very rare, in Onsala, there were only some cases per year with IPWV change more than 10 mm during 6 hours. Small, regular diurnal variations of IPWV are driven by the diurnal cycle of solar radiation linked with the evapotranspiration processes in the atmosphere and on the underlying surface, and by local air circulation.

6.3.1. Regular diurnal variability

In order to study the seasonal dependence of the regular diurnal variations in IPWV, the dataset was divided into four seasons: spring (MAM), summer (JJA), autumn (SON) and winter (DJF). For each of $N = 32$ GPS-stations their average diurnal evolution of IPWV was calculated.

Station diurnal anomalies together with the average diurnal anomalies over all stations and the average IPWV values, $\langle W \rangle$, for the entire region, are presented in Figure 8.

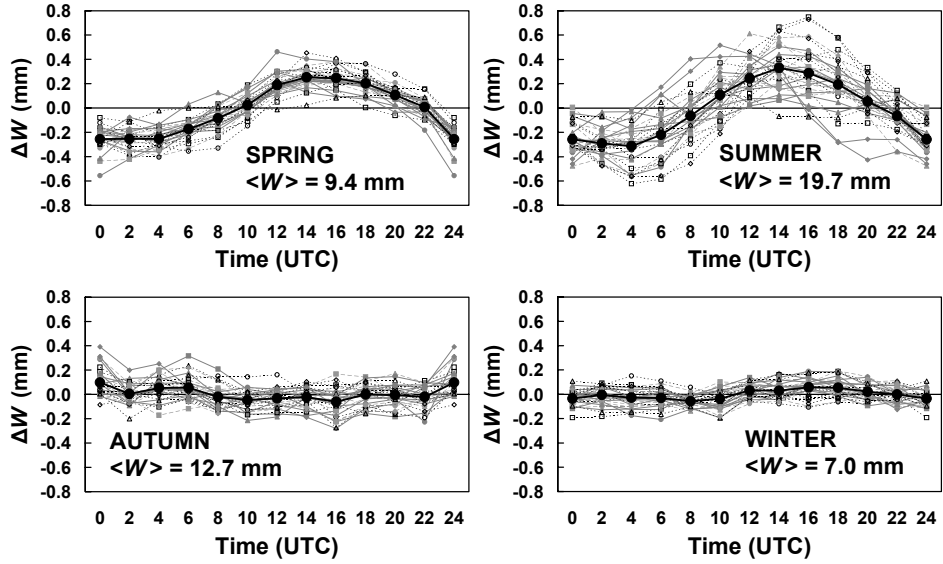


Figure 8. Grey lines: the IPWV seasonal average diurnal anomalies for the 32 GPS stations. Black lines: averages over all the 32 stations; $\langle W \rangle$ is the seasonal average of IPWV for the region (over all stations and hours).

In spring and summer the average diurnal anomaly ΔW_{UTC} has a regular, almost sinusoidal pattern (bold lines in Figure 8). The average daily cycle peaks at 14 UTC (about 15:20 Local Solar Time at the region's central meridian, 21°E) and exceeds the daily average by only 0.25 mm in spring and 0.33 mm in summer (Table 2). The lowest IPWV values typically occur between 00 and 04 UTC. They are 0.26 mm and 0.31 mm below the daily average in spring and summer respectively.

Seasonal standard deviation of the IPWV diurnal cycle is only 0.08 mm in spring and 0.16 mm in summer. These values are small compared to the average PtP values (0.51 mm for spring and 0.64 mm for summer). Thus in spring and summer, the average diurnal cycle of IPWV can be used instead of a station's individual cycle.

In autumn the average diurnal PtP value of IPWV is 0.16 mm and in winter 0.11 mm. Apparently, the smaller amplitude in the diurnal variation of incoming radiation and larger values of cloudiness in autumn and winter smooth both the temperature and the humidity differences between day and night, and therefore also the diurnal humidity cycles. The seasonal standard deviation of the IPWV diurnal cycle is 0.09 mm in autumn and 0.07 mm in winter. It seems reasonable to neglect the diurnal cycles in the IPWV in autumn and winter.

6.3.2. Extremal cases of the diurnal variability

In this section, two cases of rapid changes (decrease and increase) in the IPWV are presented. These cases represent the most extreme changes in our database for Onsala, Sweden, from 1996 to 2005.

On September 9, 1999, in 5 h 25 min (16:57–22:22 UTC) the IPWV decreased from 35 to 10 mm, i.e. by 25 mm with an average trend of about 5 mm/hour (Figure 9a). This drop can be explained by a substitution of air masses over Onsala. Vertical profiles of the specific humidity, q (g/kg), for 18 UTC and 00 UTC obtained at the nearby Landvetter airport (distance 37 km) show that during these six hours the humidity content decreased in the entire profile, especially between 1 and 4 km (Figure 10a).

The NOAA HYSPLIT model (<http://www.arl.noaa.gov/ready/hysplit4.html>) backward trajectories demonstrate the different origin of air masses over Onsala. At 18 UTC, before the fast change, hot air with high humidity content originated from Western Europe. Afterwards, at 24 UTC, cold air with low humidity content originated from Greenland, Iceland, and the North Atlantic region.

On August 10, 2000, in 6 h 20 min (00:27–06:47 UTC) the IPWV increased from 16 to 33 mm, i.e. by 17 mm with an average trend about 3 mm/hour (Figure 9b). Vertical profiles of the specific humidity, q , for 00 UTC and 12 UTC obtained at the Landvetter airport show that during 12 hours the humidity content increased along the entire profile (Figure 10b). This increase can also be explained by a long range transport of air masses: warmer and humid air from Western Europe pushed out previous colder and drier air from Greenland, Iceland, and the North Atlantic region.

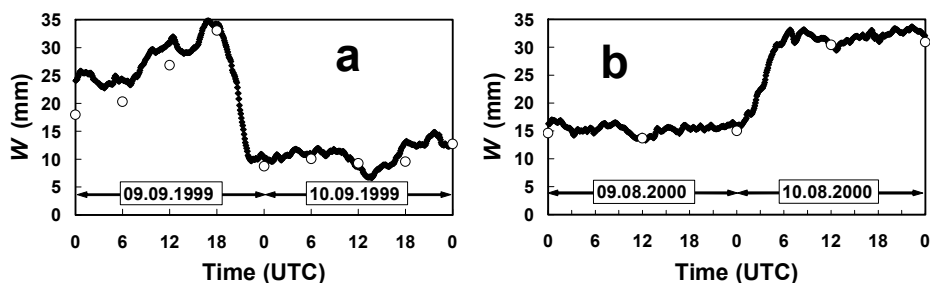


Figure 9. (a) Rapid decrease in the IPWV on September 9, 1999 and (b) increase on August 10, 2000. Diamonds represent GPS measured IPWV at the Onsala site with a temporal resolution of 5 min; circles denote IPWV measured by radiosondes at the Landvetter airport (distance 37 km).

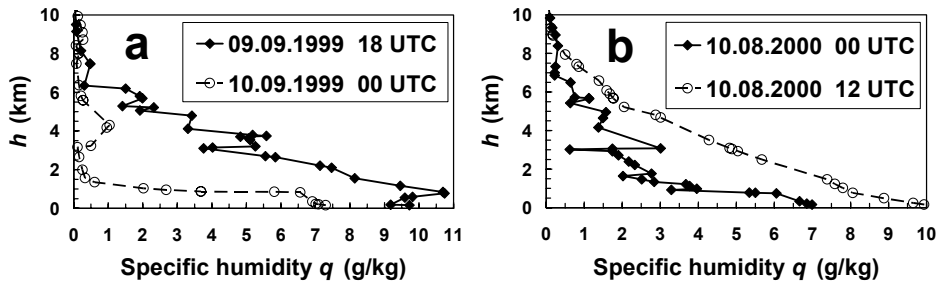


Figure 10. Vertical profiles of the specific humidity q (g kg^{-1}) at the Landvetter airport. Diamonds (connected with solid lines) show the earlier profiles before the substitution of air masses, circles (dashed lines) show the profiles for the new air masses. (a) September 9, 1999 and (b) August 10, 2000.

7. MERIDIONAL MOISTURE FLOW

The moisture transport to the Arctic is governed by the large-scale circulation patterns. The mid-tropospheric large-scale circulation in the Arctic is characterized by the polar vortex, which in winter is strong and asymmetric, with major troughs in northeastern America and eastern Asia (Serreze and Barry, 2005). The polar vortex becomes weaker and more symmetric during spring and summer. At sea level, the average winter circulation is dominated by the Icelandic Low, the Aleutian Low, and the Siberian High, while in summer the large-scale circulation is much weaker. The average meridional circulation north of approximately 50°N is related to the Polar cell characterized by ascending motion in the subpolar latitudes (50–70°N), descending motion over the pole, poleward motion aloft, and equatorward motion near the surface. The Polar cell is, however, asymmetric, much weaker, and much more disturbed by transient eddies than the Hadley and Ferrell cells. The average zonal and meridional circulations are also strongly affected by the Arctic Oscillation (Boer *et al.*, 2001).

Seasonal distribution of vertically integrated meridional moisture flux MMF is presented in row 1, Figure 11. Average seasonal average values for polar cap are from 3.2 kg m⁻¹ s⁻¹ in winter to 7.0 kg m⁻¹ s⁻¹ in summer (positive marks northward). The MMF values are highest in summer because of abundance of moisture (Sorteberg and Walsh, 2008). Major northward MMF takes place in the Atlantic section and the North Pacific Ocean. The peak northward transport in the Atlantic section is primarily due to high average specific humidities and the frequent advection of moisture by transient eddies (Serreze *et al.*, 1995a, Serreze *et al.*, 1995b). Major southward MMF takes place in the Canadian sector, especially in summer, but in total, it is much weaker than the northward transport. In all seasons, there is a notable clockwise transport of moisture around Greenland.

Seasonal contributions into yearly average moisture transport to the Arctic cap were higher in summer (36%) and autumn (26%) and lower in spring (20%) and winter (18%). These results coincide very well, within 2% in every season, with Dickson *et al.* (2000), based on rawinsonde dataset, and Sorteberg and Walsh (2008), based on NCEP/NCAR reanalysis. This supports Bromwich *et al.* (2002): all reanalyses show the same seasonal cycle in the meridional moisture transport. Satellite-based seasonal cycle for 1980–1993 found by Groves and Francis (2002) had considerably higher contribution in spring (25%), as in other seasons the contributions were some percent smaller than our values.

Seasonal interannual standard deviations of MMF and coefficients of variation of MMF are presented in Figure 11 (rows 2 and 3 respectively). Interannual standard deviations of MMF are in the same order of magnitude as the averages, the coefficient of variation is mostly in range 0.2 to 5. Seasonally, the highest interannual variability is in summer and the smallest in winter. Regionally, similarly to the MMF averages, MMF interannual variation depends

greatly on location. MMF interannual variability is higher in the Atlantic sector and the North Pacific sector with interannual standard deviation up to $15 \text{ kg m}^{-1} \text{ s}^{-1}$. The smallest interannual variability is in Greenland and in Hudson Bay: less than $3 \text{ kg m}^{-1} \text{ s}^{-1}$.

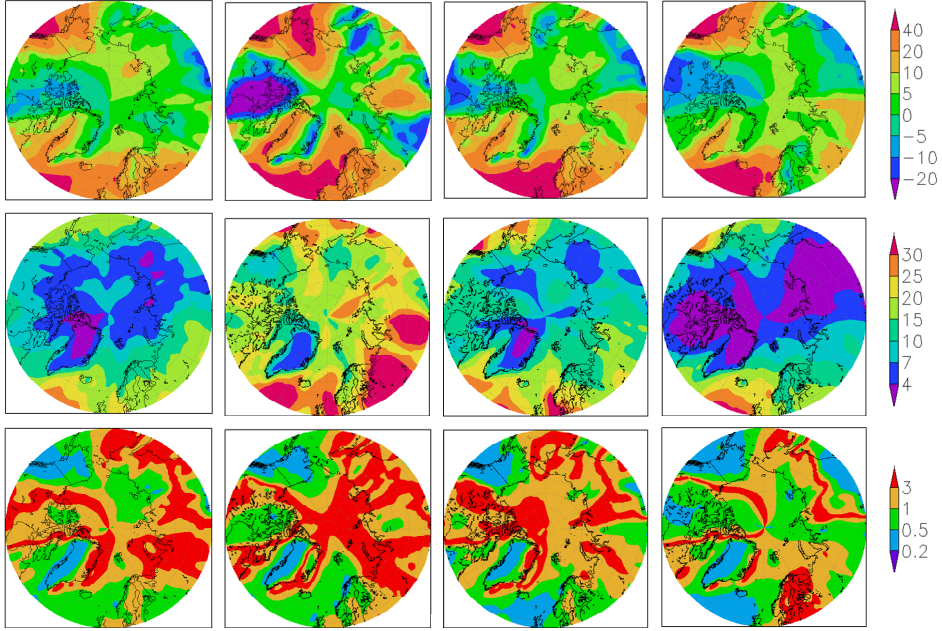


Figure 11. (row 1) Meridional moisture flux MMF ($\text{kg m}^{-1} \text{ s}^{-1}$) seasonal average, (row 2) interannual standard deviation of MMF ($\text{kg m}^{-1} \text{ s}^{-1}$) and (row 3) coefficient of variation of MMF. Columns correspond to seasons (MAM, JJA, SON and DJF). All calculations are for the period of 1979–2001, positive transport is northward.

8. CONCLUSIONS

Water vapour is the most important greenhouse gas, contributing to about 60% of the natural greenhouse effect. In contrast to other greenhouse gases, water vapour has a much higher temporal and spatial variability, which is not well observed, neither is it fully understood (Jacob, 2001, Wagner *et al.*, 2006). Precipitable water values can differ even 100 times, ranging from below 1 mm in cold and dry winter in the Polar Regions to at least 95 mm measured in India in an extremely warm and humid region. In this thesis, the author has tried to clarify precipitable water, IPWV, variability in detail for the Baltic Sea region and more generally for the region northward 55°N.

Spatial variability in the precipitable water depends generally on the latitude. This is due to the northward decrease in air temperature, which controls the atmospheric capacity to contain water vapour. In addition, spatial variability depends on orography, continentality, underlying surface type (land, water or ice), atmospheric circulation, the properties of the underlying surface, etc. (discussed in Paper D, and in Thesis Section 5). In the Baltic Sea region, seasonal average precipitable water depends mainly on the latitude, especially in transition seasons spring and autumn (discussed in Paper A, and in Thesis Section 5).

Intergovernmental Panel on Climate Change states that water vapour concentration in the atmosphere mainly depends on air temperature (IPCC, 2007). According to the ERA-40 reanalysis, however, this relation does not apply to all seasons and all regions, there were some regions with even negative correlation between IPWV and temperature in summer. As there is cold bias in the ERA-40 over the Arctic from 1979 to 1996 (Bromwich *et al.*, 2002, Bromwich *et al.*, 2007), better databases are needed for analyzing the relationship between IPWV and temperature.

Temporal variability in precipitable water has been analyzed in different time scales – seasonal, interannual and diurnal variability. Seasonal variability is the largest – the highest values of IPWV are in summer and the smallest values are in winter. For the Arctic cap region, seasonal averages differ 5 times (discussed in Paper D, and in Thesis Section 6.1). Coefficient of variation in IPWV for the region northward 55°N ranges from 5% to 10% in summer and from 10% to 20% in winter (discussed in Paper D, and in Thesis Section 6.1). Diurnal variations of IPWV have sinusoidal pattern in spring and summer with the maximum in the afternoon and the minimum after midnight. The peak to peak value for the Baltic region is 0.5 mm in spring and 0.6 mm in summer. Regular diurnal variations of IPWV are without definite pattern in autumn and winter. Besides average variability in IPWV, abrupt changes in the synoptic situation can lead to rapid and large change (more than 10 mm during several hours) in the IPWV. However, these kinds of abrupt changes are very rare: in Onsala, there were only some cases per year with IPWV change more than 10 mm during 6 hours (discussed in Paper B, and in Thesis Section 6.2).

For better understanding of moisture movements, vertically integrated meridional moisture flux, MMF, was analyzed. The MMF seasonal average values for polar cap range from $3.2 \text{ kg m}^{-1} \text{ s}^{-1}$ in winter to $7.0 \text{ kg m}^{-1} \text{ s}^{-1}$ in summer. The MMF values are highest in summer because of the abundance of moisture. Interannual standard deviations of MMF are in the same order of magnitude as the averages, the coefficient of variation is mostly in range of 0.2 to 5. Major northward MMF takes place over the Atlantic and Pacific Oceans. The peak northward transport in the Atlantic sector is primarily due to high average specific humidity and the frequent advection of moisture by transient eddies. Major southward MMF takes place in the Canadian sector, especially in summer, but in total, it is much weaker than the northward transport in the Atlantic sector. Seasonal contributions to the yearly average moisture transport into the Arctic cap were higher in summer (36%) and autumn (26%), and lower in spring (20%) and winter (18%) (discussed in Paper D, and in Thesis Section 7).

The results of this thesis are as follows:

- Accuracy in radiosonde measured IPWV is estimated to be 8% at the confidence level 95%. Thus for the average value $\text{IPWV} = 25 \text{ mm}$, expanded uncertainty is 2 mm, equal to accuracy estimations for GPS-measured IPWV.
- It has been shown for the Baltic Sea region that the three methods (radiosonde, GPS, ERA-40) for IPWV are in reasonably good agreement with each other.
- The isolines of IPWV are prolonged in the Canada-Siberia axes during all seasons, with the maximum asymmetry in winter, when the heat and moisture sources in the Atlantic and Pacific Oceans ensure the high level of IPWV.
- Intergovernmental Panel on Climate Change states that water vapour concentration in the atmosphere mainly depends on air temperature. According to the ERA-40 reanalysis, however, this relation does not apply to all seasons and all regions. As there is cold bias in the ERA-40 over the Arctic from 1979 to 1996, better databases are needed for the relationship between IPWV and temperature.
- The isolines of IPWV in the Baltic Sea region are quite zonal and uniformly distributed.
- Parameterization equation for seasonal average IPWV from the latitude degree for the Baltic Sea region is given.
- Parameterization equation for present IPWV from surface water vapour pressure and the latitude degree for the Baltic Sea region is given.
- Temporal variability is divided into three components – seasonal, interannual and diurnal components. The highest component is seasonal variability – the difference between IPWV summer and winter averages is from 2 times to 11 times, depending on locations. The highest seasonal

variability in IPWV is in Yakutsk region and the smallest is in the Scottish region.

- Coefficients of interannual variations of IPWV range from 5% to 10% in summer and from 10% to 20% in winter.
- Diurnal average cycle in the IPWV is sinusoidal in spring and summer with peak to peak values of 0.5–0.6 mm. In autumn and winter, there is no clear diurnal cycle in the IPWV.
- Abrupt changes in the synoptic situation can lead to rapid and large change (more than 10 mm during several hours) in the IPWV.
- Major northward MMF takes place over the Atlantic and Pacific Oceans, major southward MMF takes place in the Canadian sector, especially in summer, but in total, it is much weaker than the northward transport in the Atlantic sector.
- Inter-annual standard deviations of MMF are in the same order of magnitude as the averages, the coefficient of variation is mostly in range of 0.2 to 5.

9. SUMMARIES OF APPENDED ARTICLES

Paper A: Jakobson E, Ohvriil H, Okulov O, Laulainen N. 2005. Variability of radiosonde-observed precipitable water in the Baltic region. *Nordic Hydrology* **36**: 423–433.

Availability of surface humidity data allows a much better approximation of the IPWV already using a linear function of surface water vapour pressure, e_0 , and geographical latitude, φ . Standard deviations of this two-parameter approximation are considerably smaller compared with the one-parameter approximation. The standard deviations are 3.3–4.6 mm in summer (18–22% of the summer average) and 2.0–3.4 mm in winter (31–34%). In cases when more precise methods for the evaluation of IPWV (radiosounding, solar photometry, GPS, microwave radiometry) are not available, this approximation can be recommended for optical studies of atmospheric aerosol content. This approximation can also be used for compiling retrospective time series of IPWV even for historical periods when radiosondes were not yet available.

Paper B: Jakobson E, Ohvriil H, Elgered G. 2009. Diurnal variability of precipitable water in the Baltic region, impact on transmittance of the direct solar radiation. *Boreal Environmental Research* **14**: 45–55.

Diurnal variations of IPWV can be separated into two groups – the large irregular and small regular ones. The large variations in IPWV are related to changes in the synoptic situation and the substitution of air masses above the location of observations. As shown by the analysis of two extreme examples of abrupt changes in atmospheric humidity at the Onsala site, the IPWV total increase/decrease can reach even 25 mm during six hours. Concerning the Onsala site, there were only some cases per year with IPWV change in the IPWV that was larger than 10 mm during six hours.

The average diurnal variability of the IPWV in the Baltic region, between 56–70°N, is low, the maximal average station PtP value is in summer 1.4 mm at Borås. The seasonal average diurnal variation of IPWV has a sinusoidal pattern in spring and summer with the maximum in the afternoon and the minimum after midnight. The PtP value, for the region average IPWV cycle, is 0.5 mm in spring and 0.6 mm in summer. Regular diurnal variations of IPWV are without a definite pattern in autumn and winter, PtP values of the average IPWV cycle are only 0.1–0.2 mm.

Paper C: Vihma T, Jaagus J, Jakobson E, Palo T. 2008. Meteorological conditions in the Arctic summer 2007 as recorded on the drifting ice station Tara. *Geophysical Research Letters* **35**: L18706. DOI:10.1029/2008GL034681.

This work is based on meteorological measurements in 35 Russian “North Pole” drifting stations (hereinafter called as “NP stations”) since the 1930s, in field campaign SHEBA (Surface Heat Budget of the Arctic Ocean) (Uttal *et*

al., 2002) during 1997–1998, and in the drifting ice station Tara (Gascard *et al.*, 2008) during 2006–2007.

As SHEBA was located further south, the most interesting comparisons were those between Tara and the NP stations. The observations indicated that the melting season in the Arctic Ocean was at least twice as long at Tara in 2007 than at the NP stations on average. This was preceded by a warm spring: 2 m air temperature in April 2007 was 7.0°C higher than the NP station mean. The July mean 2 m air temperature was equal (−0.2°C) at Tara and the NP stations. This is related to the fact that the surface and 2°m air temperatures are closely coupled via the sensible heat flux and longwave radiation (Vihma and Pirazzini, 2005). If the air temperature tends to rise above 0°C, the heat will be used in melting snow and ice. If the air temperature tends to drop well below 0°C, the leads and melt ponds start to freeze, and the release of the latent heat will reduce the decrease of the air temperature. Hence the near-surface air temperature remains close to 0°C throughout the melting season, and is not a sensitive indicator for the climate change in the central Arctic, while the length of the melting season is a better indicator.

In summer 2007 at Tara, at least at the altitudes of approximately 200–1000 m, the Arctic atmosphere was warmer than at the NP stations in 1954–1985: at the height of 500 m the difference was 0.9°C. Taking into account the mean spatial temperature gradient between the locations of Tara and the NP stations, the temporal change has probably exceeded 1°C. On the basis of the ERA-40 re-analysis, Graverson *et al.* (2008) concluded that in summers 1979–2001 the maximum climate warming in the Arctic took place at the altitudes of approximately 2–4 km. In the lowermost 1 km, Graverson *et al.* (2008) found a summer warming of 0.1–0.3°C per decade. Accordingly, both their and our studies suggest that the major Arctic warming in summer has taken place well above the ice surface. This urgently calls for more observations on the vertical structure of the atmosphere over the Arctic Ocean.

Paper D: Jakobson E, Vihma T. 2009. On the atmospheric moisture budget in the Arctic according to ERA-40 reanalysis. *International Journal of Climatology*. Submitted.

Variability in IPWV seasonal averages depends significantly on location. Higher (more than 5 times) variability is in zone covering Canada except the Rocky Mountains, Arctic Ocean and Siberia. Highest variability – more than 11 times – is in Yakutsk region, where in summer the average value exceeds 20 mm, while in winter the average value is 1–2 mm. Smaller (less than 5 times) variability is above Atlantic Ocean, Europe, southern Greenland, the Bering Sea and the Rocky Mountains in Alaska and Canada. Smallest variability – less than 2 times – is in Scotland region, where all seasonal averages are in the range of 10–20 mm.

Transition seasons IPWV averages are relatively very similar, autumn values are 1.3 ± 0.2 times higher than spring ones in whole area (Figure 6b). This

shows that local factors do not play important role in transition seasons IPWV proportion, quite independently of the latitude, underlying surface type etc.

The MMF values are highest in summer because of abundance of moisture. Major northward MMF takes place over the Atlantic and Pacific Oceans. The peak northward transport in the Atlantic sector is primarily due to high average specific humidities and the frequent advection of moisture by transient eddies. Major southward MMF takes place in the Canada sector, especially in summer, but totally, it is much weaker than the northward transport in the Atlantic sector. In all seasons, there is notable clockwise transport of moisture around Greenland.

10. SUMMARY IN ESTONIAN

“Atmosfääri niiskussisalduse ajalis-ruumiline muutlikkus”

Veeaur on kõige olulisem kasvuhoonegaas, andes ligikaudu 60% kasvuhoone efektist. Veeaur on erinevalt teistest kasvuhoonegaasidest ajaliselt ja ruumiliselt palju muutlikum, see on aga siiani korralikult läbi uurimata.

Taandatud veekihi paksuseks ehk sadestatavaks veeauruks (*Integrated Precipitable Water Vapour*, IPWV) nimetatakse veehulka, mille võib saada vertikaalses atmosfäärisambas sisalduva kogu veeauru kondenseerimisel, ühikuks $\text{kg}\cdot\text{m}^{-2}$. Arvuliselt vastab sellele veekihi paksus millimeetrites. IPWV väärtused võivad varieeruda isegi 100 korda – minimaalsed väärtused on külma ja kuiva ilmaga alla 1 mm, maksimaalne teadaolev väärtus on aga 95 mm, mõõdetud India väga sooja ja niiskes piirkonnas. Käesolevas doktoritöös on uuritud IPWV muutlikkust Läänemere piirkonnas ning üldisemalt vööndis 55. laiuskraadist põhja pool.

Sadestatava veeauru ruumiline varieeruvus sõltub üldiselt laiuskraadist – kõrgematel laiuskraadidel on madalam temperatuur ning õhku ”mahub” vähem veeauru. Lisaks sõltub see veel orograafiast, aluspinna tüübist (maismaa, vesi, jää), õhu tsirkulatsioonist jne. Läänemere piirkonnas sõltub sadestatava veeauru keskmine sesoonne väärtus peamiselt laiuskraadist, eriti ülemineku aasta-aegadel, kevadel ja sügisel.

Valitsustevahelise kliimamuutuste paneeli IPCC väitel sõltub sadestatava veeauru hulk atmosfääris peamiselt õhutemperatuurist. ERA-40 tagasianalüüsi mudeli põhjal aga see väide ei kehti kõikidel aasta-aegadel kõikides piirkondades: suvel esineb isegi alasid, kus korrelatsioon sadestatava veeauru ning temperatuuri vahel on negatiivne. Kuna ERA-40 temperatuurandmetes on Arktika piirkonnas aastatel 1979 kuni 1996 süstemaatiline viga, on sadestatava veeauru ning temperatuuri vahelise seose analüüsimiseks vaja paremaid andmebaase.

Sadestatava veeauru ajalist muutlikkust on antud töös analüüsitud erinevates ajaskaalades – ööpäevad, sesoonid ning aastad. Kõige suurem on sesoonne muutlikkus – vööndis 70. laiuskraadist põhja pool erinevad sesoonsed keskmised väärtused 5 korda. Aastatevaheline IPWV variatsioonikoefitsient on vööndis 55. laiuskraadist põhja pool suvel enamasti 5% kuni 10% ja talvel 10% kuni 20%. IPWV kevadine ja suvine ööpäevane varieeruvus on sinusoidaalne, maksimumiga pärastlõunal ning miinimumiga pärast südaööd. Läänemere piirkonnas on ööpäevase varieeruvuse amplituud kevadel 0,5 mm ja suvel 0,6 mm. Sügisel ja talvel puudub IPWV selge ööpäevane käik. Ilma järsu muutuse korral võib aga IPWV väärtus muutuda ka üle 10 mm ainult mõne tunni jooksul. Siiski, muutuseid üle 10 mm 6 tunni jooksul toimub väga harva, Onsalas (Rootsi) ainult mõned korrad aastas.

Niiskuse horisontaalse transpordi mõistmiseks uuriti vertikaalselt integreeritud keskmist meridionaalset niiskuse voogu (Mean Meridional Flux, MMF). MMF sesoonsed keskmised väärtused piirkonnas 70. laiuskraadist põhja

pool on vahemikus $3,2 \text{ kg m}^{-1} \text{ s}^{-1}$ talvel kuni $7,0 \text{ kg m}^{-1} \text{ s}^{-1}$ suvel. MMF väärtused on suurimad suvel, sest siis on kõige rohkem niiskust. Aastatevaheline MMF standardhälve on samas suurusjärgus tema keskväärtusega, variatsioonikoefitsient on enamasti 0,2 kuni 5. Peamine põhjasuunaline niiskuse transport toimub Atlandi ookeani ja Vaikse ookeani sektorites. Atlandi sektori suur niiskuse transpordi maksimum on põhjustatud kõrgest keskmisest niiskusest ning sagedasest niiskuse adveksioonist mittestatsionaarsete keeriste poolt. Peamine lõunasuunaline niiskuse transport toimub Kanada sektoris, kuid on palju väiksem kui põhjasuunaline transport Atlandi sektoris. Sesoonsed panused aasta keskmisesse niiskuse transporti 70. laiuskraadist põhja poole on suuremad suvel (36%) ja sügisel (26%) ning väiksemad kevadel (20%) ja talvel (18%).

Doktoritöö tulemused:

- Raadiosondiga mõõdetud sadestatava veeauru IPWV suhteliseks täpsuseks usaldusnivool 95% oleme hinnanud 8%. Keskmise väärtuse $\text{IPWV} = 25 \text{ mm}$ puhul on seega laiendmääramatus 2 mm, sama suureks on hinnatud ka GPS meetodil mõõdetud IPWV laiendmääramatus.
- Kolme meetodiga (raadiosond, GPS ja ERA-40) saadud IPWV on Läänemere regioonis omavahel heas kooskõlas.
- IPWV isojooned on kõikidel aastaegadel Kanada-Siberi sihis välja venitatud. Maksimaalne asümmeetria on talvel, kuna Atlandilt ja Vaiksest ookeanilt pärinev soojus ning niiskus hoiab IPWV väärtusi kõrgel.
- Valitsustevahelise kliimamuutuste paneeli IPCC väitel (IPCC, 2007) sõltub IPWV hulk atmosfääris peamiselt õhutemperatuurist. ERA-40 tagasianalüüsi mudeli põhjal aga see väide ei kehti kõikidel aastaegadel kõikides piirkondades. Kuna ERA-40 temperatuuriandmetes on Arktika piirkonnas aastatel 1979 kuni 1996 süstemaatiline viga, on IPWV ning temperatuuri vahelise seose analüüsimiseks vaja paremaid andmebaase.
- Läänemere regioonis on IPWV isojooned üsna võõndilised ning ühtlaselt jaotunud.
- Läänemere regiooni jaoks on leitud laiuskraadist sõltuv parameteriseerimisvalem sesoonikeskmise IPWV leidmiseks.
- Läänemere regiooni jaoks on leitud maapealsest veeaururõhust ning laiuskraadist sõltuv parameteriseerimisvalem IPWV hetkeväärtuse leidmiseks.
- IPWV ajalist muutlikkust on analüüsitud erinevates ajaskaalades – ööpäevad, sesoonid ning aastad. Sesoone varieeruvus on kõige suurem, erinevus IPWV suviste ja talviste väärtuste vahel on sõltuvalt piirkonnast 2 kuni 11 korda. Suurim sesoonse muutlikkuse piirkond on Jakuutia piirkonnas, väikseim Šotimaa piirkonnas.
- Aastatevaheline IPWV standardhälve on võõndis 55. laiuskraadist põhja pool enamasti suvel 5% kuni 10% ja talvel 10% kuni 20%.

- IPWV ööpäevane käik on kevadel ja suvel sinusoidaalne, amplituudiga 0,5–0,6 mm. Sügisel ja talvel puudub IPWV selge ööpäevane käik.
- Ilma järsu muutuse korral võib IPWV väärtus muutuda väga kiiresti (üle 10 mm mõne tunni jooksul).
- Peamine põhjasuunaline niiskuse transport toimub Atlandi ookeani ja Vaikse ookeani sektorites, peamine lõunasuunaline niiskuse transport toimub Kanada sektoris, kuid on palju väiksem kui põhjasuunaline transport Atlandi sektoris.
- Aastatevaheline niiskuse transpordi standardhälve on samas suurusjärgus tema keskväärtusega, variatsioonikoefitsient on enamasti 0,2 kuni 5.

REFERENCES

1. Antikainen V, Paukkunen A, Jauhiainen H. 2002. Measurement accuracy and repeatability of Vaisala RS90 radiosonde. *Vaisala News* **159/2002**: 11–13.
2. Aoki T, Aoki T, Fukabori M, Uchiyama A. 1999. Numerical simulation of the atmospheric effects on snow albedo with a multiple scattering radiative transfer model for the atmosphere-snow system. *Journal of the Meteorological Society of Japan* **77**: 595–614.
3. Aruksaar H, Liidemaa H, Martin I, Mürk H, Nei I, Põiklik K. 1964. *Üld- ja agrometeoroloogia (General and Agrometeorology)*. Eesti Raamat: Tallinn.
4. Boer GJ, Fourest S, Yu B. 2001. The signature of the annular modes in the moisture budget, *Journal of Climatology* **14**: 3655–3665.
5. Bouma HR, Stoew B. 2001. GPS observations of daily variations in the atmospheric water vapor content. *Physics and Chemistry of the Earth Part A* **26(6–8)**: 389–392.
6. Bromwich DH, Fogt RL, Hodges KI, Walsh JE. 2007. A tropospheric assessment of the ERA-40, NCEP, and JRA-25 global reanalyses in the polar regions. *Journal of Geophysical Research* **112**: D10111 1–21. DOI:10.1029/2006JD007859.
7. Bromwich DH, Wang S-H, Monaghan AJ. 2002. ERA-40 representation of the Arctic atmospheric moisture budget. *ERA-40 Project Report Series* **3**. ECMWF: Reading, UK.
8. Dai A, Wang J, Ware RH, Hove T. 2002. Diurnal variation in water over North America and its implications for sampling errors in radiosonde humidity. *Journal of Geophysical Research* **107**. DOI:10.1029/2001JD000642.
9. Dickson RR, Osborn TJ, Hurrell JW, Meincke J, Blindheim J, Adlandsvik B, Vinje T, Alekseev G, Maslowski W. 2000. The Arctic Ocean Response to the North Atlantic Oscillation. *Journal of Climate* **13**: 2671–2696.
10. Emardson TR, Derks HJP. 2000. On the relation between wet delay and the integrated precipitable water vapour in the European atmosphere. *Meteorological Applications* **7**: 61–68. DOI:10.1017/S1350482700001377.
11. Emardson TR, Elgered G, Johansson J. 1998. Three months of continuous monitoring of atmospheric water vapor with a network of Global Positioning System receivers. *Journal of Geophysical Research* **103**: 1807–1820.
12. Gradinarsky LP, Johansson JM, Bouma HR, Scherneck H-G, Elgered G. 2002. Climate monitoring using GPS. *Physics and Chemistry of the Earth* **27**: 335–340.
13. Graversen RG, Mauritsen T, Tjernström M, Källen E, Svensson G. 2008. Vertical structure of recent Arctic warming. *Nature* **541**: 53–56.
14. Groves DG, Francis JA. 2002. Variability of the Arctic atmospheric moisture budget from TOVS satellite data. *Journal of Geophysical Research – Atmospheres* **107(D24)**: Art. No. 4785.
15. Güldner J, Spänkuch D. 1999. Results of year-round remotely sensed integrated water vapor by groundbased microwave radiometry. *Journal of Applied Meteorology* **38**: 981–989.
16. Güldner J. 2001. Validation of integrated water vapor using independent measurement techniques. *Physics and Chemistry of the Earth Part A* **26**: 427–431.
17. IPCC 2007. Climate change 2007: the physical science basis. Contribution of working group I to the fourth assessment report of the Intergovernmental Panel on Climate Change. Cambridge University Press: Cambridge and New York.

18. Jacob D. 2001. The role of water vapour in the atmosphere. A short overview from a climate modeller's view. *Physics and Chemistry of the Earth Part A* **26**: 523–527.
19. Johansson JM, Davis JL, Scherneck H-G, Milne GA, Vermeer M, Mitrovica JX, Bennett RA, Jonsson B, Elgered G, Elosegui P, Koivula H, Poutanen M, Rönäng BO, Shapiro II. 2002. Continuous GPS measurements of postglacial adjustment in Fennoscandia 1. Geodetic results. *Journal of Geophysical Research* **107**. DOI:10.1029/2001JB000400.
20. Kaleschke L, Lüpkes C, Vihma T, Haarpaintner J, Bochert A, Hartmann J, Heygster G. 2001. SSM/I sea ice remote sensing for mesoscale ocean-atmosphere interaction analysis. *Canadian Journal of Remote Sensing* **27**: 526–536.
21. Kirkup L, Frenkel B. 2008. *An Introduction to Uncertainty in Measurement*. Cambridge University Press: Cambridge.
22. Lidberg M, Johansson JM, Scherneck H-G, Davis JL. 2007. An improved and extended GPS-derived 3D velocity field of the glacial isostatic adjustment (GIA) in Fennoscandia. *Journal of Geodesy* **81**: 213–230. DOI: 10.1007/s00190-006-0102-4.
23. Maurellis A, Tennyson J. 2003. The climatic effects of water vapour. *Physics World May*: 29–33.
24. Mietus M. 1998. The climate of the Baltic Sea basin. *WMO, Marine Meteorology and Related Oceanographic Activities*: **41**. WMO/TD-No. 933.
25. Okulov O, Ohvril H, Kivi R. 2002. Atmospheric precipitable water in Estonia, 1990–2002. *Boreal Environmental Research* **7**: 291–300.
26. Peixoto JP, Oort AH. 1992. *Physics of Climate*. American Institute of Physics: New York.
27. Reitan CH. 1960. Mean monthly values of precipitable water over the United States, 1946–56. *Monthly Weather Review* **88**: 25–35.
28. Rinke A, Melsheimer C, Dethloff K, Heygster G. 2008. Arctic total water vapor: comparison of regional climate simulations with observations, and simulated decadal trends. *Journal of Hydrometeorology*. DOI: 10.1175/2008JHM970.1.
29. Ross RJ, Elliott WP, Seidel DJ. 2002. Lower-tropospheric humidity-temperature relationships in radiosonde observations and atmospheric general circulation models. *Journal of Hydrometeorology* **3**: 26–38.
30. Serreze MC, Barrett AP, Slater AG, Steele M, Zhang J, Trenberth KE. 2007. The large-scale energy budget of the Arctic. *Journal of Geophysical Research* **112**: D11122. DOI: 10.1029/2006JD008230.
31. Serreze MC, Barrett AP, Slater AG, Woodgate RA, Aagaard K, Lammers RB, Steele M, Moritz R, Meredith M, Lee CM. 2006. The large-scale freshwater cycle of the Arctic. *Journal of Geophysical Research* **111**(C11). DOI:10.1029/2005JC003424.
32. Serreze MC, Barry RG, Rehder MC, Walsh JE, Drewry D. 1995a. Variability in atmospheric circulation and moisture flux over the Arctic. *Philosophical Transactions: Physical Sciences and Engineering* **352**: 215–225.
33. Serreze MC, Barry RG, Walsh JE. 1995b. Atmospheric water vapour characteristics at 70°N. *Journal of Climate* **8**: 719–731.
34. Serreze MC, Barry RG. 2005. *The Arctic Climate System*. Cambridge University Press: Cambridge.

35. Serreze MC, Etringer AJ. 2003. Precipitation characteristics of the Eurasian Arctic drainage system. *International Journal of Climatology* **23**: 1267–1291.
36. Simmons AJ, Hollingsworth A. 2002. Some aspects of the improvement in skill of numerical weather prediction. *Quarterly Journal of the Royal Meteorological Society* **128**: 647–677.
37. Sorteberg A, Katsov V, Walsh J, Palova T. 2007. The Arctic surface energy budget as simulated with the IPCC AR4 AOGCMs. *Climate Dynamics* **29**: 131–156. DOI:10.1007/s00382-006-0222-9.
38. Sorteberg A, Walsh JE. 2008. Seasonal cyclone variability at 70°N and its impact on moisture transport into the Arctic. *Tellus* **60A**: 570–586. DOI:10.1111/j.1600-0870.2008.00314.x.
39. Tietäväinen H, Vihma T. 2008. Atmospheric moisture budget over Antarctica and the Southern Ocean based on the ERA-40 reanalysis. *International Journal of Climatology*. DOI: 10.1002/joc.1684.
40. Tregoning P, Boers R, O'Brien D, Hendy M. 1998. Accuracy of absolute precipitable water vapor estimates from GPS observations. *Journal of Geophysical Research* **103**: 701–710.
41. Trenberth KE, Smith L. 2005. The mass of the atmosphere: a constraint on global analyses. *Journal of Climate* **18**: 864–875. DOI:10.1175/JCLI-3299.1.
42. Trenberth KE, Fasullo J, Smith L. 2005. Trends and variability in column-integrated atmospheric water vapor. *Climate Dynamics* **24**: 741–758. DOI:10.1007/s00382-005-0017-4.
43. Uppala SM, Kållberg PW, Simmons AJ, Andrae U, da Costa Bechtold V, Fiorino M, Gibson JK, Haseler J, Hernandez A, Kelly GA, Li X, Onogi K, Saarinen S, Sokka N, Allan RP, Andersson E, Arpe K, Balmaseda MA, Beljaars ACM, van deBerg L, Bidlot J, Bormann N, Caires S, Chevallier F, Dethof A, Dragosavac M, Fisher M, Fuentes M, Hagemann S, H'olm E, Hoskins BJ, Isaksen L, Janssen PAEM, Jenne R, McNally AP, Mahfouf J-F, Morcrette J-J, Rayner NA, Saunders RW, Simon P, Sterl A, Trenberth KE, Untch A, Vasiljevic D, Viterbo P, Woollen J. 2005. The ERA-40 re-analysis. **131**: 2961–3012. DOI: 10.1256/qj.04.176.
44. Uttal T, Curry JA, Mcphee MG, Perovich DK, Moritz RE, Maslanik JA, Guest PS, Stern HL, Moore JA, Turenne R, Heiberg A, Serreze MC, Wylie DP, Persson OG, Paulson, Halle C, Morison JH, Wheeler PA, Makshtas A, Welch H, Shupe MD, Intrieri JM, Stamnes K., Lindsey RW, Pinkel R, Pegau WS, Stanton TP, Grenfeld TC. 2002. The surface heat budget of the Arctic Ocean. *Bulletin of the American Meteorological Society* **83**: 255–275.
45. Vihma T, Pirazzini R. 2005. On the factors controlling the snow surface and 2-m air temperatures over the Arctic sea ice in winter. *Boundary-Layer Meteorology* **117**: 73–90.
46. Wagner T, Beirle S, Grzegorski M, Platt U. 2006. Global trends (1996–2003) of total column precipitable water observed by Global Ozone Monitoring Experiment (GOME) on ERS-2 and their relation to nearsurface temperature. *Journal of Geophysical Research* **111**: D12102. DOI:10.1029/2005JD006523.
47. Walsh JE, Zhou X, Portis D, Serrese MC. 1994. Atmospheric Contribution to Hydrologic Variations in the Arctic. *Atmosphere-Ocean* **32(4)**: 733–755.
48. WMO (1988). *Technical Regulations vol. 1* General Meteorological Standards and Recommended Practices Appendix B, 1-Ap-B-3. World Meteorological Organisation: Switzerland.

ACKNOWLEDGEMENTS

Firstly, I would like to thank my high school physics teacher Aarne Lillemaa for guiding me to physics.

I am very thankful to my supervisor, Assoc. Prof. Hanno Ohvril, for his continuous attention and support. Without his straightforward way of supervision during the last 7 years, from my BSc studies, I would not have been in a position to write these Acknowledgements at all.

Very special thanks to my colleagues from the Institute of Environmental Physics, especially Prof. Rein Rõõm and Assoc. Prof. Piia Post.

I am greatly indebted to Prof. Jaak Jaagus from Institute of Geography for inviting me to project DAMOCLES, and for good teamwork.

Thanks for practical knowledge and support to my colleagues in the Testing Centre: Olev Saks, Martin Vilbaste, Ivo Leito, Koit Herodes, Vladimir Shor.

I am highly grateful for my international collaborations with Timo Vihma from the Finnish Meteorological Institute and Gunnar Elgered from the Onsala Space Observatory. It is really constructive to work with such experienced and helpful people.

I wish to thank Külli Teder for correcting the English manuscript.

I would like to thank my family for support, encouragement and patient.

Finally, I would like to thank You for reading this thesis.

CURRICULUM VITAE

Name: Erko Jakobson
Date of birth: 16. January 1979
Marital status: married, 2 children
Phone: +37 256 643 946
E-mail: erko.jakobson@ut.ee



Education

- 2004– PhD studies in Environmental Physics, University of Tartu.
2002–2004 MSc in Physics, University of Tartu. MSc thesis: ‘Parameterization of water vapour in the Baltic Sea region’.
1997–2002 BSc in Physics, University of Tartu. BSc thesis: ‘Characteristic of precipitable water by Finnish meteostations’

Installation of a sensor on tether-line on packice. Arctic Ocean field work in April 2007, 88th parallel.
Photo courtesy of Francis Latreille.

Lecture courses

- Fundamentals of the Environmental Physics II, 3 ECTS, in Estonian.
- Measurement Data Processing, 3 ECTS, in English.

Employment

- 2008– University of Tartu, Faculty of Science and Technology, Institute of Physics; Engineer
2006–2008 University of Tartu, Faculty of Biology and Geography, Institute of Geography, Chair of Physical Geography and Landscape Ecology; Extraordinary Researcher
2005–2008 University of Tartu, Faculty of Physics and Chemistry, Testing Centre; Engineer

Field of research

Natural Sciences and Engineering, environmental physics. Temporal and spatial variations of water vapour in the atmosphere, humidity transport.

Participation in grants & projects

- Development of methods for physical analysis of column water vapour and aerosol content for investigation of environmental situation in the Baltic Sea region (grant no. 7347, 2008–2011).

- Investigation of columnar content of water vapour and aerosols (grant no. 5857, 2004–2007).
- Development of the numerical weather prediction towards the forecasting of atmospheric environment (Project SF0180038s08, 2008–2013).
- Landscape changes in Estonia related to global climate warming and human activity (Project SF0180049s09, 2009–2014).
- Estonian contact person of European Association of National Metrology Institutes (EURAMET) Technical Committee FLOW.

Visiting scholarships and fieldworks

- The Centre for Metrology and Accreditation (MIKES) and in the Technical Research Centre of Finland (VTT, Finland), February 2004 (2 weeks). Host: Dr. M. Heinonen, training on calibration of anemometers and hygrometers.
- Westenberg Engineering (Germany), March 2004 (3 days). Host Dr. J. Westenberg, manufacturer training of wind tunnel.
- Max-Planck-Institut für Meteorologie (Germany), May 2005 (2 weeks), Host: Prof. D. Jacob, Comparison between model and sunphotometer-measured values of precipitable water.
- Onsala Space Observatory (Sweden), Sep 2005 (2 weeks) and Apr 2006 (2 weeks), Host: prof. G. Elgered, diurnal variations of GPS-measured precipitable water.
- EURAMET TC FLOW meetings in Greece 2005, Portugal 2006 and Turkey 2007.
- Arctic Ocean field work August 2006 (1 month) within the DAMOCLES project, installation of meteorological instruments (meteomast, radiation mast, sonic anemometers) on pack ice; instruction of crew.
- Arctic Ocean field work April 2007 (2 weeks) within the DAMOCLES project, reformation of meteorological instruments on pack ice, atmosphere vertical profiling.

CURRICULUM VITAE IN ESTONIAN

Nimi: Erko Jakobson
Sünniaeg: 16. jaanuar 1979
Perekonnaseis: abielus, 2 last
Telefon: +37 256 643 946
E-post: erko.jakobson@ut.ee

Haridus

2004– Doktorantuur, TÜ Keskkonnanfüüsika Instituut.
2002–2004 MSc füüsikas (keskkonnanfüüsika), TÜ: „Atmosfääri veeauru-
sisalduse parametrizeerimine Läänemere regioonis“.
1997–2002 BSc füüsikas, TÜ: „Atmosfääri veesisalduse parametri-
seerimine Sodankylä ja Jokioise andmete alusel”.

Loengukursused

- Keskkonna füüsika alused II, 3 ECTS.
- Mõõtmisandmete töötlemine, 3 ECTS, inglise keeles.

Teenistuskäik

2008– Insener, TÜ, Füüsika Instituut.
2006–2008 Erakorraline teadur, TÜ, Geograafia Instituut.
2005–2008 Insener, TÜ, Tartu Ülikooli Katsekoda.

Peamised töösuunad

Veeauru ajaline ja ruumiline muutlikkus atmosfääris, niiskuse transport.

Osalemine grantides ja projektides

- Atmosfäärisamba veeauru ja aerosoolisisalduse füüsikalise analüüsi meetodite arendamine Läänemere piirkonna keskkonnaseisundi uurimiseks (grant nr 7347, 2008–2011).
- Õhusamba veeauru- ja aerosoolisisalduse uurimine (grant nr 5857, 2004–2007).
- Numbrilise ilmaennustuse arendamine õhukeskkonna prognooside suunas (Projekt SF0180038s08, 2008–2013).
- Maastiku muutused Eestis seoses globaalse kliima soojenemise ja inimtegevusega (Projekt SF0180049s09, 2009–2014).
- Eesti kontaktisik Euroopa riiklike metroloogiainstituutide assotsiatsiooni (EURAMET) tehnilises komitees ”Voolamised” (FLOW).

Stažeerimine ja välitööd

- Anemomeetrite ning hügromeetrite kalibreerimise koolitus Soomes Metroloogia ja Akrediteerimise Keskuses (MIKES) ja Soome Tehnikauurimise Keskuses (VTT), 2004 veebruar (2 nädalat).
- Tuuletunneli tehasekoolitus Saksamaal firmas Westenber Engineering, 2004 märts (3 päeva).
- Mudeli tulemuste võrdlemine päikesefotomeetriga mõõdetud sadestatava veeauruga Saksamaal Max-Plancki Meteoroloogiainstituudis, 2005 märts (2 nädalat).
- GPS-meetodil mõõdetud sadestatava veeauru ööpäevase varieeruvuse uurimine Rootsisis Onsala Kosmoseobservatooriumis 2005 september (2 nädalat) ja 2006 aprill (2 nädalat).
- EURAMET voolamise (FLOW) töögrupi koosolekud Kreekas 2005, Portugalis 2006 ja Türgis 2007.
- Välitöö Põhja-Jäämere jääl – meteoroloogiliste instrumentide (meteomast, kiirgusmõõdjate mast ja helilaine-anemomeetrid) jääle paigaldamine ning meeskonna instrueerimine – projekti DAMOCLES raames 2006 augustis (1 kuu).
- Välitöö Põhja-Jäämere jääl – meteoroloogiliste instrumentide korrastamine ning atmosfääri vertikaalne sondeerimine – projekti DAMOCLES raames 2007 aprillis (2 nädalat).

DISSERTATIONES GEOPHYSICALES UNIVERSITATIS TARTUENSIS

1. **Andres Kuusk.** The hot-spot effect in plant canopy reflectance. Tartu, 1991.
2. **Tiit Nilson.** Radiative transfer in non-homogeneous plant canopies. Tartu, 1991.
3. **Helgi Arst.** Atmosfääri ja mere kiirguskarakteristikud looduskeskkonna seisundi informaatoritena (vene keeles). Tartu, 1991.
4. **Juha Sarkkula.** Measuring and modelling water currents and quality as a part of decision making process for water pollution control. Tartu, 1992.
5. **Piia Post.** On the two radiatively effective cloud parameters. Tartu, 1993.
6. **Aadu Mirme.** Electric aerosol spectrometry. Tartu, 1994.
7. **Aare Luts.** Mathematical simulation of the evolutions of air ions. Tartu, 1995.
8. **Tiit Kutser.** Estimation of water quality in turbid inland and coastal waters by passive optical remote sensing. Tartu, 1997.
9. **Ülle Kikas.** Atmospheric aerosol in the Baltic region. Tartu, 1998.
10. **Tarmo Kõuts.** Processes of deep water renewal in the Baltic sea. Tartu, 1999.
11. **Anu Reinart.** Underwater light field characteristics in different types of Estonian and Finnish lakes. Tartu, 2000.
12. **Marko Kaasik.** Parameterisation of atmospheric boundary layer in the numerical model of air pollution transport. Tartu, 2000.
13. **Janek Laanearu.** Topographically constrained deep-water flows in channels. Tartu, 2001.
14. **Urmas Raudsepp.** Wind-driven circulation in the gulf of Riga. Tartu, 2001.
15. **Urmas Hõrrak.** Air ion mobility spectrum at a rural area. Tartu, 2001.
16. **Marko Vana.** Formation and evolution of atmospheric aerosol size spectrum by the occurrence of nucleation burst events in the atmospheric boundary layer; transport of the climatically active particulate air pollution. Tartu, 2002.
17. **Veljo Kimmel.** Analysis of methods of air quality assessment. Applications in Estonia. Tartu, 2002.
18. **Oleg Okulov.** Variability of atmospheric transparency and precipitable water in Estonia. Tartu, 2003.
19. **Aarne Männik.** Implementation and validation of the nonhydrostatic adiabatic core of the numerical weather prediction model hirlam. Tartu, 2003.
20. **Matti Mõttus.** Shortwave solar radiation field inside willow canopy. Tartu, 2004.
21. **Kalev Rannat.** Long weakly nonlinear waves in geophysical applications. Tartu, 2007.
22. **Rigel Kivi.** Observations of ozone, polar stratospheric cloud and water vapour profiles in the arctic. Tartu, 2007.